STUDY ON FATIGUE OF HYBRID PLATE GIRDERS UNDER CONSTANT MOMENT

by

J. Yinh
A. A. Toprac

Research Report Number 96-3

Fatigue Strength of Hybrid
Plate Girders Under Shear
Research Project Number 3-5-66-96

conducted for

The Texas Highway Department

in cooperation with the
U.S. Department of Transportation
Federal Highway Administration
Bureau of Public Roads

by the

CENTER FOR HIGHWAY RESEARCH
THE UNIVERSITY OF TEXAS
AUSTIN, TEXAS

January 1969

ACKNOWLEDGMENTS

This investigation is part of the hybrid plate girder research being conducted at The Structures Fatigue Research Laboratory, Balcones Research Center, The University of Texas at Austin, Center for Highway Research under the administration of Dr. John J. McKetta. This work was sponsored by the Texas Highway Department and the Bureau of Public Roads. The interest and financial support of the sponsor and encouragement of the Texas Plate Girder Supervisory Committee are gratefully acknowledged. The study was supervised by Dr. A. A. Toprac.

The opinions, findings, and conclusions expressed in this publication are those of the authors and not necessarily those of the Bureau of Public Roads.

This is the third of four reports that describes the work in Research Study No. 3-5-66-96, entitled "Fatigue Strength of Hybrid Plate Girders Under Shear." The first report issued is Report No. 96-1, entitled "Additional Fatigue Tests of Hybrid Plate Girders Under Pure Bending Moment." The second report was entitled "Fatigue Tests of Hybrid Plate Girders Under Combined Bending and Shear." The fourth report will be prepared and issued after the completion of tests presently under way.

ABSTRACT

Fatigue tests of four hybrid plate girders comprised of ASTM A514 steel flanges and ASTM A36 steel web under constant moment condition are reported. For all the girders the web was 36 in. deep. Two girders had a slenderness ratio of 197 while the same for the other two was 267. All four girders were subjected to a stress range of 30 ksi with a maximum applied stress of 50 ksi.

The purpose of this investigation was to collect necessary data to study the behavior of hybrid plate girders in the region of high stress range and relate the results with the available test data in lower stress ranges.

The test results are presented and discussed in comparison with previous test data. A limited statistical analysis is made in an attempt to find the influence of parameters which affect the fatigue life of hybrid plate girders. Several design criteria based on the test results and empirical analyses are suggested.

Test results showed that by limiting certain variables, the secondary bending stresses in the web can be reduced so that their effect will not be enough to produce fatigue cracks in the compression side of the girders. However, cracks will appear in the tension side due to other factors such as notches due to fabrication and various stress concentrations.

The regression analyses have shown that fatigue cracks in the high stress range region will occur after a larger number of cycles than suggested in previous reports. Though most of the factors involved are interrelated, it is shown that, it is possible to consider only one of the main parameters to derive an approximate relationship for the number of cycles required to produce a crack.

TABLE OF CONTENTS

CHAPTER Page

LIST OF TABLES

LIST OF FIGURES

1. INTRODUCTION

1.1 Background

A combination of high strength and carbon steels in structural members can result in a more economical and efficient design. This is particularly true with plate girders, where the use of constructional alloy steel (ASTM 514) in the severely stressed flanges would increase the load capacity of the member, while a carbon steel (ASTM 36) web provides the resistance for shear. Thus, such a combination of steels results in an overall light and, consequently economical section.

1.2 Previous Tests

Because of the fast growing use of hybrid plate girders, a program to study both the static and fatigue strength of these structural elements was started at The University of Texas.

The study presented herein will be limited to the fatigue behavior of welded hybrid plate girders under constant moment. Previous tests[1] have included both panel size and full-size specimens with varying stress ranges (σ_R) and extreme stresses (σ_{max} and σ_{min}). Table 1 shows a summary of these tests.

The most significant conclusions on this continuing research in fatigue of hybrid plate girders can be summarized as follows:

1. Fatigue strength of welded hybrid plate girders cannot be directly related to that of homogeneous ones, because of the existence of yielding in the web at its extremities next to the flanges in the first type of girders mentioned.
2. Secondary bending stresses caused by lateral web deflections have a decisive effect on the fatigue life.
3. For specimens subjected to applied stresses below the yield point of the web material, no cracks were found within two million cycles.
4. Fabrication irregularities can strongly reduce the fatigue life.
5. Fatigue life of a girder subjected to combined bending and shear is shorter than when under pure bending only.
6. In hybrid plate girders under combined bending and shear, fatigue cracks appeared earlier at the tip of transverse stiffeners cut shorter than usual, because of their inability to limit web deflections.

1.3 Purpose and Scope

Recommendations for design have been suggested based on previous studies. However, no information on girders subjected to a high stress range was available from these studies. Since extrapolation is not acceptable in fatigue data analysis,[2] a test program consisting of four hybrid plate girders subjected to a stress range of 30 ksi, was designed.

This report presents the test results of these four hybrid plate girders and compares them to previous test data. Some of the factors

which influence the fatigue behavior of these girders were investigated. Considerations are given to the secondary bending stresses at the flange-to-web juncture. Boundary conditions between flanges and web are also analyzed. Finally, a statistical study is presented of all the data available.

1.4 Nomenclature

N	=	number of cycles to a crack appearance.
P_{cr}	=	load which produces buckling (kips).
P_{max}	=	maximum applied load during fatigue test (kips).
P_{min}	=	minimum applied load during fatigue test (kips).
P_y	=	load which produces general yielding in the web (kips).
t	=	web thickness (in.).
α	=	aspect ratio, ratio of panel length to web depth.
β	=	slenderness ratio, ratio of web depth to web thickness.
$(\delta_o)_{max}$	=	maximum initial lateral web eccentricity.
$(\delta_{oc})_{max}$	=	maximum initial lateral web eccentricity on the compression side of the web.
σ_{cr}	=	elastic buckling stress in bending (reduced) (ksi).
σ_{max}	=	maximum stress, the highest algebraic value of the stress in the cycle. In this report, it refers to the stress at the extreme fiber of the flanges at maximum load.
σ_{min}	=	minimum stress, the lowest algebraic value of the stress in the cycle. In this report, it refers to the stress at the extreme fiber of the flanges at minimum load.
σ_R	=	stress range, the algebraic difference between the maximum and minimum stresses in a cycle.
σ_y	=	static yield stress.
σ_{yw}	=	yield stress of web.

2. SPECIMENS AND TEST SETUP

2.1 Specimen Designation

The specimens have been labelled in such a way that characteristic information can be read from their designations.

Each girder is designated in the following way:

a) The first figure indicates the thickness of the web plate in sixteenths of an inch.

b) The next two digits represent the minimum stress, in ksi, to which the specimen is subjected during the pulsating period.

c) In a similar way, the next two numbers designate the maximum applied stress in ksi.

d) The letter following the numbers identifies the test series. An "R" at the end indicates a duplicate test on a specimen with parameters identical to those of the original specimen.

For example, 3 20 50 DR, designates that the specimen had a web thickness of 3/16 in. and that the minimum and maximum applied stresses were 20 and 50 ksi, respectively. Further, that it is a duplicate of the "D" series specimen 32050 D.

2.2 Description of Specimens

The four specimens reported herein are:

22050D* 22050DR* 32050D 32050DR

Figure 1 shows the dimensions and details of the tested girders which had 8 in. x 1/2 in. flanges except 32050DR, for which the same were 7 1/2 in. x 1/2 in. All flanges were of ASTM A514 and the webs of A36 steel. The stiffeners at load and reaction points were made of A514 steel while all intermediate stiffeners were made of A36 steel.

The flanges were fillet welded to the web using submerged automatic arc welding, with full penetration required. For all the stiffeners, E6018 electrodes were used.

2.3 Design Considerations

The only geometric parameter studied in the investigation was the web slenderness ratio, β. To have different β ratios without changing any other geometric variable, all the dimensions were kept constant, except the thickness of the web. The two slenderness ratios studied in this investigation were 267 and 197. Both were above the 165 required by the AASHO[3] bridge specifications for A36 steel.

Except the end bearing stiffeners, all stiffeners were cut two inches from the tension flange to reduce the possibility of premature fatigue crack in the tension flange. All four specimens had two test panels in the middle (Fig. 1). A narrow panel on each side of the test

*Actual thickness of this specimen was 10 gage. The designation "2" (1/8 in. thickness) was chosen because it is the closest approximation in terms of sixteenths of an inch.

panels was provided to reduce local effects from the applied loads. To reduce vertical deflections, 3/16 in. web material was used outside the test panels. These 3/16 in. plates were welded to the 10 gage web by means of two 45^{o} splices (see Fig. 1).

2.4 Material Properties

Physical properties were checked in the laboratory by testing tensile coupons obtained from the same plates used in the fabrication of the girders. Physical properties obtained by coupon tests are compared in Table 2 with those from the mill report supplied by the manufacturer. It is necessary to note that the measured yield stress values given in the table are the static yield stress of the material.

2.5 Reference Loads

Actual dimensions and measured material properties were used to compute reference loads for each girder (Tables 2 and 3). The tests were designed so that at maximum load the extreme fibers of the flange were stressed to 50 ksi, and at the minimum load, 20 ksi, resulting in a stress range of 30 ksi.

Table 4 is a summary of these calculations. The theoretical critical values computed according to Reference (4), with modulus of elasticity of 29,500 ksi and Poisson's ratio of 0.3, are incorporated in Table 4. The second column shows the critical web buckling stress in bending for the test panels adjusted for the flange stress reduction suggested in Reference (4). The third column gives the respective loads to produce these stresses. The ratios P_{max}/P_{cr} and P_{min}/P_{cr} are also shown for reference in the same table.

2.6 Test Setup

Figure 2 is a sketch of a typical test setup. The girders were simply supported and were subjected to two symmetrical equal loads at the locations shown. The dynamic loads were applied by a pulsator and hydraulic jacks of 120 kips dynamic capacity each, and at a constant speed of approximately 250 cycles per minute. During the test sufficient lateral supports were used to prevent any tilting of the specimen.

The coordinate system for each panel to be used throughout this report is also illustrated in Fig. 2. The origin is at the geometric center of each panel. The positive directions of this coordinate system is toward the right for X, upwards for Y and normal to the web and towards the reader for Z. The plane contained by the points lying in the positive Z direction will be called near side (N. S.), while the points on the opposite side, far side (F. S.). Also shown in Fig. 2 are the shear and bending moment diagrams. Figure 3 shows a general view of a typical test setup.

2.7 Instrumentation

Vertical deflections were measured at the supports and at mid-span. Lateral web deflections were obtained at zero, minimum and maximum loads at 3 in. by 3 in. grid points as shown in Fig. 4.

The locations of electrical resistance strain gages (SR-4, Type A5-S6) used in the flanges of each test panel are shown in Fig. 5. The main purpose of these strain gages was to check the response of the girder under the static load. Flange rotations of the test panels were

measured under static load. A set of dial gages at 12 in. intervals was used to measure the flange rotation, as shown in Fig. 6.

To get an indication of loss of stiffness during the fatigue cycling, vertical deflections were measured with a slip gage placed at the center-line of the specimen as shown in Fig. 7.

The girders were whitewashed prior to testing. Under static load, yield lines are detected easier because of the whitewash, while under fatigue load, it facilitates the visual inspection and detection of cracks.

2.8 Repairs of Fatigue Cracks

Cracks formed at the tension side of the girder were repaired to continue testing. The cracks were first gouged out by the "arc-air" method, and the new weld was deposited. Depending on whether the repair was made on the tension flange or at the juncture of the web and stiffener, AWS E11018 or E7018 low hydrogen electrodes were used.

To avoid stress concentrations, all repairs on the tension flange were ground smooth after welding. The repairs made at the juncture of the web and stiffener were not ground.

3. TEST PROCEDURE AND RESULTS

3.1 General

The test sequence and procedure for each girder is as follows:

1. Initial static test: the girder was loaded to P_{max}, the maximum load of the subsequent fatigue test; it was then unloaded to the minimum load (P_{min}) and finally to zero load. Pertinent readings were taken at several load intervals in each stage of loading.
2. The fatigue test: the girder was subjected to sinusoidal pulsating load. Visual inspections were made throughout the test to detect initiation of cracks and to record their propagation. The cracks were numbered according to the order of discovery. Slip gage readings were taken at each inspection period to check for loss of stiffness.

3.2 Static Test Results

Typical static test results are briefly presented in this section. A typical load vs. centerline deflection curve (Girder 32050D) is shown in Fig. 8. A theoretical line based on elastic theory is also incorporated.

Two different behaviors of the top flange rotations were observed in the test. In girder 22050D the top flange of each of the test panels

rotated in directions opposite to each other, as Fig. 9a illustrates. For girder 32050D the flange of the two test panels rotated in the same direction, as shown in Fig. 9b. In girder 32050DR the top flange behaved similarly to girder 32050D. No such measurements were made for girder 22050DR.

Measured strains on the top flange of girder 32050DR, are compared with theoretical values in Fig. 10. This close agreement between experimental results and elastic theory was obtained in the other girders also.

Lateral web deflection contours and deflected profiles for one of the test panels of girder 22050D are shown in Fig. 11 for zero P_{min} and P_{max} loads. Similar results were obtained with the rest of the specimens.

3.3 Fatigue Test Results

A brief description of the test results for each girder studied is reported below. A summary of the test results is presented in Table 5. The details of cracks developed in each specimen are shown in Figs. 12 through 15. Unless otherwise noted the figures show the near side (positive Z direction) of the specimens.

It should be noted here, that although all cracks developed during the testing, irrespective of location, are indicated in Table 5 and Figs. 12 to 15, only those between the load points are considered in the discussions or are used in the analyses which are presented in subsequent sections of this report.

3.3.1 Girder 22050D (Fig. 12)

The first crack, observed in test panel T-1, was along the toe of the top flange-web fillet weld. It was observed only on the near side, at 230,000 cycles. At 257,000 cycles, the crack propagated to the far side.

Crack 2, along the stiffener-web weld in S13 (see Table 5) was discovered at 450,000 cycles. This crack was repaired at 456,000 cycles and in an attempt to stop its reappearance a stiffener was welded as shown by a dashed line in Fig. 12. However, as testing was resumed, the crack reopened after 88,000 additional cycles and testing was terminated. At the completion of the test this crack was 7 7/8 in. long.

At the end of the test, a final inspection revealed cracks 3 and 4, which were similar to crack 2, and crack 5 located at the middle of panel T-1 at its tension side. Crack 5, which started at a discontinuity in the weld, had penetrated through the bottom flange.

3.3.2 Girder 22050DR (Fig. 13)

Cracks 1 and 2 were observed at 532,000 and 543,000 cycles. At 560,000 cycles, crack 3 was detected. Crack 4 was found only in the near side, at 609,000 cycles, while crack 5 appeared on the far side, at 615,00 cycles, at which time testing was terminated because crack 3 propagated extensively in the tension flange.

3.3.3 Girder 32050D (Fig. 14)

The only crack found in this specimen was observed at 496,000 cycles. Testing was stopped and as the crack was being repaired a

hole of approximately 1/4 in. round, probably due to a slip in the automatic welding process, was discovered (see detail in Fig. 14).

After resuming the test the crack reappeared at 566,000 cycles. Because of its quick propagation, at 571,540 cycles the test was terminated.

3.3.4 Girder 32050DR (Fig. 15)

This specimen was a replica of 32050D except for the dimensions of the flanges (Table 3). Crack 1, along the bearing stiffener-to-web weld, appeared on the near side at 439,000 cycles and extended to the far side at 487,000 cycles. At 527,000 cycles, cracks 2 and 3 were detected and found to be 3 1/8 in. and 2 1/4 in. long respectively. These three cracks were repaired and testing was resumed. Cracks 4 and 5, which are similar to 1 and 2, were noted at 560,000 cycles on the other side of the stiffener. The test was discontinued at 656,720 cycles.

4. DISCUSSION

4.1 Fatigue Cracks

The fatigue cracks found in this investigation can be grouped in three distinctive types, as has been already reported in Reference 1. These cracks are classified as type 1, 2, or 3, depending on their locations and nature. A test panel which depicts the three crack types is shown in Fig. 16. All cracks observed on the specimens tested are indicated in Table 5 and their type is noted.

Type 1 cracks appear at the toe of the compression flange-to-web fillet weld, in the heat affected zone of the web. They are caused by the secondary bending stresses produced by the lateral movements of the web during the fatigue cycling (1) (5). Because of their nature, these cracks will be studied in conjunction with the web behavior and secondary bending stresses in section 4.2.

Type 2 cracks start at the stiffener-to-web juncture, at the cutoff end of transverse stiffeners, and produce complete failure after reaching the tension flange. Their cause is considered to be the local stress concentration due to the abrupt termination of stiffeners. Because type 2 cracks are located in the tension side of the girder their propagation is faster than that of type 1 cracks. This can be seen by comparing Figs. 17 and 18 where typical propagation rates for type 1

and type 2 cracks are shown. The propagation of type 2 cracks was not easily controllable. Every time these cracks were discovered, the test was stopped and they were repaired using the technique explained in section 2.8. After testing was resumed, the cracks appeared again in the same locations, or at places affected by the repairs. For this reason, the type 2 cracks are classified as dangerous.

The type 3 cracks developed in three of the four girders tested were always observed in the tension flange-to-web juncture.* High weld porosity or discontinuity due to stopping and starting the welding were the cause of these cracks. Because of their location in the tension side these cracks have a high rate of growth (see Fig. 19) leading to complete failure after penetrating into the tension flange. Attempted repairs of these cracks were proved to be unsuccessful because they reappeared in the same place after a small number of additional cycles. These cracks are detrimental to the overall fatigue life of the girder.

Considering fabrication irregularities as the main factor for the formation of type 3 cracks, it is logical to expect a scatter in the experimental results. However, the numbers of cycles at which type 3 cracks were first observed in three of the four specimens were very close to each other: 544,000, 560,000 and 566,000 cycles, respectively.

4.2 Web Behavior and Secondary Bending Stresses

Due to the high slenderness ratio of the panels, it is logical to expect initial lateral eccentricity in the web. The shape of the initial

*Type 3 cracks can develop at the edge of the flange also (Ref. 1 and 6).

profiles varied according to the slenderness ratio of the panel. For very slender webs, the initial deformations will usually produce a double or triple curvature profile, while a stockier web will generally have a single curvature profile, as indicated in Reference 6. The measured magnitudes of these initial out-of-plane eccentricities varied from 0.001 in. to 0.255 in., indicating that they can be as much as 2 times the thickness of the web.

As the girder is loaded, the compression above the neutral axis increases and the tension below the neutral axis decreases these deflections. This web behavior is typical in constant moment panels, as illustrated in Fig. 20, where a cross section profile is shown at zero, minimum and maximum load. As it can be seen in this figure, even a reversal of the curvature can be expected during the two limiting stages (P_{max} and P_{min}) of the cyclic loading.

These lateral movements of the web in the Z axis direction, because of the rigidity of the boundary elements of the test panel (flanges and stiffeners), produce bending stresses in the web. These stresses are known as secondary bending stresses. An implication that there is some fixity between web and flanges can be deducted from the fact that close to the flange-to-web juncture the deflected web shape showed a point of inflection (9), noticeable also in Fig. 20.

The flexing action of the web due to the cycling between P_{max} and P_{min} eventually produces type 1 cracks in the juncture of the compression flange and web, where the secondary bending stresses are more critical. No type 1 crack should be expected in the tension side of girders, because of the gradual decrease of the web deflection below

the neutral axis under loading, producing a release on these stresses in the tension side.[5] The numbers of cycles a girder can stand before the appearance of type 1 cracks will depend on factors such as the initial web deflections, web slenderness ratio, applied loads, and rigidity of the boundaries.

To find the degree of fixity between flanges and web, flange rotations were measured during the static test (see Figs. 9a and b). The variation of these rotations along the x-axis direction of the panels is illustrated in Fig. 21. No dial gages were installed at the top flange over the outer stiffeners of panels T-1 and T-2. The rotations at these points were assumed to be the same as at the top of the stiffener common to both test panels, which has been found by considering a linear variation between points B and C (see Fig. 21).

By means of finite difference techniques, with a 3 in. mesh points, the magnitudes of the secondary bending stresses along the top flange-to-web juncture were calculated, first considering the measured flange rotations and then assuming no rotation of flange. A typical result of these computations can be seen in Fig. 22, where the variation of these stresses is compared for the two cases mentioned above. It is evident that the difference between the two cases is negligible. The difference between the two cases at the vicinity of the largest lateral eccentricities is only about 1%. From this it is logical to conclude that the web-flange boundaries could be considered rigid.

Another feature that should be noted in Fig. 22 is that type 1 cracks appeared only on those locations where the secondary bending stress exceeded the web yield stress, as in panel T-1 (girder 22050D, Fig. 22), where the critical secondary bending stress was 60% higher than the web

yield stress. In panel T-2, the critical secondary stress was just about equal to the yield stress of the web, and no type 1 crack was found during the fatigue test. Thus, a criterion for the prevention of type 1 cracks would be that the critical secondary bending stresses should not exceed the yield stress of the web material.

4.3 Initial Web Deflection

On the knowledge that the initial deflected shape of the web and its magnitude have a definite influence on the secondary bending stresses, an analysis intended to find a limiting value of the maximum initial lateral web deflections was made. This analysis, carried out using the typical elements shown in Fig. 23, was based on the finite difference approach. The derivation to obtain the final expression given below is presented in Appendix A and the equation numbers mentioned herein after will refer to those in the same appendix.

$$\frac{\delta_o}{t} \leq 1000 \frac{\sigma_{yw}}{E} \qquad \text{(A-19)}$$

Although equation (A-19) relates the limiting value of $\frac{\delta_o}{t}$ to the yield strain of the web material only, results have given good correlation, as can be seen in Fig. 24, where the parameter

$$\frac{\text{Actual } [\delta_o]_{max}}{\text{Limiting } [\delta_o]_{max}}$$

for all the girders reported here and in Reference 1 has been plotted with respect to number of cycles.

Actual $[\delta_o]_{max}$ refers to the maximum measured initial deflection and Limiting $[\delta_o]_{max}$ indicates the limiting maximum initial

deflection as computed by equation (A-19). Since it has been found that no crack will appear within two million cycles if the maximum applied stress is lower than the yield stress of the web, [1] only those panels subjected to higher stress than the yield stress of the web material were considered. The points in circles represent those corresponding to the girders where type 1 cracks were observed, while the cross points are those with no cracks. The actual crack points were plotted at the number of cycles when they were first observed, while those points with no cracks were presented at the number of cycles when the test was stopped. A semilogarithmic scale was used to encompass all the points. It can be seen that in no case a panel having a $\left[\delta_o\right]_{max}$ less than the one given by equation (A-19) had type 1 cracks. Based on these results, it is possible to state that equation (A-19) gives conservative values and may be used as a lower bound for limiting the maximum initial lateral web eccentricities on a girder subjected to fatigue under pure bending. However, it is necessary to point out here that this limiting value is not enough to prevent type 1 cracks as other parameters should also be considered. Values of

$$\frac{\text{Actual } \left[\delta_o\right]_{max}}{t}$$

for the studied specimens can be found in Table 6, which will be used later for the regression analysis.

4.4 Slenderness Ratio

Reference 1, where 36 in. deep hybrid plate girders were tested under pure bending, reported that type 1 cracks were found only in the

specimens having a web thickness of 3/16 in. or less, (see Table 6). In the four girders tested in this program type 1 cracks were observed only in the two with 10 gage web thickness.

Since all the girders mentioned above were 36 in. deep, a 3/16 in. web thickness can be related by the slenderness ratio β, which would be 192. Such a value may be considered as a limiting slenderness ratio to prevent type 1 cracks. This value is just 13% higher than the slenderness ratio of 165 suggested by the AASHO Specifications.[3] However, since the β ratio given by AASHO is dependent on the web yield stress, the value of 192 suggested above should be used in conjunction with equation (A-19) to have at least an indirect relationship between the slenderness ratio and yield stress of the web material.

At this stage, it is imperative to note, from Tables 1 and 6, that only one, the 32550B, of all girders with 3/16 in. web thickness reported had a type 1 crack. This fact leads to the consideration that the β ratio of 192 suggested above is a low value, or, at least, a conservative value, since most probably the type 1 crack in specimen 32550B was due to other factors rather than due to β. In fact, by examining Table 6, it can be seen that the maximum δ_o/t of this girder is the largest among 3/16 in. web-girders.

4.5 Stress Level

Only on those specimens where the maximum applied stress was above the web yield stress were fatigue cracks observed;[1] for all other girders whose maximum applied strains did not exceed the yield strain of the material of the web at its extremities, it was possible to reach two million cycles or more without any crack.

This behavior can be explained by the fact that although the flange strains are in the elastic range, the web, since it is partially yielded, would fluctuate under cyclic loading in both the elastic and the inelastic ranges. The partially yielded condition of the web will make the secondary bending stresses critical and eventually produce type 1 cracks. If that yielded depth of the web is deep enough to include the cutoff points of the transverse stiffeners on the test panels, the stress concentration produced by the abrupt termination of the stiffeners would be in the inelastic range, provoking the type 2 cracks. Also, stress concentrations due to weld discontinuities are critical and initiate type 3 cracks in the tension flange. From this it can be concluded that to prevent fatigue crack below 2 million cycles the maximum applies stress should be less than the yield stress of the web material.

4.6 Effect of Fatigue Cycling on Static Behavior

At 496,000 cycles, after the first crack (type 3) was observed in specimen 32050D, and before it was repaired, an additional static test up to P_{max} was made to study the effect of fatigue cycling in the overall behavior of the girder. No significant difference was found in the response of the girder when compared with the behavior during the initial static test. Figure 25 shows the lateral web movements at the center ($x = 0.0$) of the test panel T-1 for the cases before the application of cyclic loading and after 496,000 cycles. It is apparent that the panel behaved the same way in both cases. So it can be assumed that, if all the fatigue cracks are repaired, a girder which has been subjected to fatigue cycling will have a static strength similar to an identical girder with no previous fatigue history.

4.7 Regression Analysis

Multiple regression analyses, using the data of this report and those from Reference 1, as shown in Table 6, were made to find some statistical relationships between the fatigue strength, represented by the number of cycles* before an initial crack was observed, and the following parameters:

$$\left[\frac{\delta_o}{t}\right]_{max}, \left[\frac{\delta_{oc}}{t}\right]_{max}, \sigma_{min}, \sigma_{max}, \sigma_R, \beta, \text{ and } \frac{\sigma_{max}}{\sigma_{cr}}$$

Cracks are recorded in Table 6 according to their type and the number of cycles at which they were first observed. The column designated as "first crack" registers either run-outs or the cycles at which the first crack was discovered irrespective of the type of crack.

The non-dimensional parameter $\left[\frac{\delta_{oc}}{t}\right]_{max}$ which is the ratio of the maximum initial lateral web eccentricity in the compression side of the girder to the web thickness, was used to compare the $\left[\delta_{oc}\right]_{max}$ of the various girders tested. This ratio was included in the analyses as a recognition of the fact that with increasing loads, the web lateral deflections increase in the compression side. The ratio $\frac{\sigma_{max}}{\sigma_{cr}}$ was obtained using the critical buckling stress (σ_{cr}) given by Basler.[4] Irrespective of the theoretical mode of failure, that is, vertical or torsional buckling, the minimum σ_{cr} was selected for the above ratio.

---

*The dependent variable throughout the analyses was the number of cycles (N) that a specimen withstood before a crack was first observed.

4.7.1 Determination of the Regression Line

A linear relationship between the logarithms of the parameters and of the dependent variable were assumed in the analyses as given below:

$$\log N = C + C_1 \log X_1 + C_2 \log X_2 + \ldots\ldots + C_n \log X_n$$

where N is the number of cycles to initial crack and $X_1 \ldots\ldots X_n$ are the various parameters mentioned in section 4.7, while C, C_1, C_n are coefficients to be determined by the least square approach.

The regression analysis[10] was carried out in a stepwise manner using a Fortran computer program.[11] A sequence of multiple regression equations was obtained. At each step one variable was added to the regression equation and its effect was checked. The variable added was the one which had the highest "F" ratio. Also, variables were automatically removed when their "F" ratios became too low. Throughout the analysis, a significance level of 0.01 was used to check whether a variable should be included, while a 0.005 significance level was considered adequate for the removal of a variable.

4.7.2 Initial Cracks

It was assumed that two million cycles was the maximum that any member of a bridge would have in its useful life. Thus, the behavior of the girders after two million cycles was not of interest in this study. Hence, for the purpose of the regression analysis, the girders that lasted more than two million cycles, (run-out specimens) were considered to have a fatigue life of two million cycles.

All the parameters were considered in a first analysis to get a correlation for the number of cycles to the first crack, irrespective of what type of crack it was. The results of this analysis indicates that σ_{max} and σ_R were more important than the other parameters. A second regression analysis was than carried out including only the above two parameters. Each of the above analyses was carried out:

a) With the run-out specimens considering $N = 2 \times 10^6$.

b) Without the run-out specimens.

The final equations thus obtained for the above two cases are respectively:

$$\log (N \times 10^{-3}) = 0.08 \log \sigma_{max} - 1.56 \log \sigma_R + 4.89 \qquad (4\text{-}1)$$

$$\log (N \times 10^{-3}) = -1.20 \log \sigma_{max} - 1.03 \log \sigma_R + 6.27 \qquad (4\text{-}2)$$

Equation (4-1) can be expressed as:

$$\log (N \times 10^{-3}) = 4.89 - 1.56 \log \sigma_R \qquad (4\text{-}3)$$

since the coefficient of σ_{max} is negligible when compared with the coefficient of σ_R.

Equation (4-3) is plotted in Fig. 26. Actual test points from Reference 1 and the present study are also shown in this figure.

A similar procedure was used to analyze the data for type 1, type 2 and type 3 cracks separately, considering their respective number of cycles. The resulting equations are:

Type 1 cracks:

$$\log (N \times 10^{-3}) = 4.78 - 2.18 \log \sigma_R \qquad (4\text{-}4)$$

Type 2 cracks:

$$\log (N \times 10^{-3}) = 8.16 - 3.22 \log \sigma_{max} \qquad (4\text{-}5)$$

Type 3 cracks:

$$\log (N \times 10^{-3}) = 6.81 - 2.37 \log \sigma_{max} \qquad (4\text{-}6)$$

These three equations are plotted in Figs. 27, 28 and 29, respectively. In these figures, the corresponding equations for type 1 and type 2 cracks from Reference (1) are also plotted for comparison.

It should be noted that equation (9) of Reference 1 (see Fig. 28) was derived for σ_R = 25 ksi only. However, the two points obtained from the present study (with σ_R = 30 ksi) showed good correlation with both equations plotted in Fig. 28. Therefore, when stress ranges of 25 to 30 ksi are considered either of the equations could be used. It should also be noted in Figs. 27, 28 and 29 that for high stress ranges, the regression equations derived in this report indicate a longer fatigue life than by using the equations of Reference 1. However, with low stress ranges, the opposite is true, that is, the regression equations of Reference 1 are a more conservative estimate of the fatigue life than those derived here.

5. CONCLUSIONS

The discussion and analyses of the results of hybrid plate girders subjected to fatigue under pure bending, in conjunction with previous data, have led to the following conclusions:

1. Actual flange rotations during fatigue cycling have a negligible effect on the secondary bending stresses. For all practical purposes, it can be assumed that flanges do not rotate while the girders are subjected to repeated loads.
2. Type 1 cracks will appear at locations along the toe of the compression flange-to-web fillet weld, whenever the secondary bending stress, due to web lateral movements, is higher than the yield stress of the web material.
3. The effect of secondary bending stresses may be controlled and type 1 cracks avoided by limiting initial web eccentricity δ_o as follows:

$$(\delta_o/t)_{max} \leq 1000\ \sigma_{yw}/E$$

4. Considering fatigue, the web depth-to-thickness ratio requirement for plate girders, specified by AASHO, seems to be a conservative value.

5. With cracks repaired, a plate girder previously subjected to fatigue will have a static strength equivalent to an identical girder with no previous fatigue history.
6. Fatigue cracks located in the tension side of the girders, that is, type 2 and type 3 cracks, could not be successfully repaired using the available welding operator and procedure used in section 3.2. Shortly after each repair, cracks did reappear at the same locations.
7. Fatigue life of hybrid plate girders subjected to high stress range (σ_R = 30 ksi) is longer than that suggested in Reference 1.
8. Although more data are necessary to support the statistical analyses presented herein, some reasonable estimates about the appearance and type of the first fatigue crack can be obtained from the equations formulated in this report.

APPENDIX A

DERIVATION OF LIMIT VALUE FOR THE MAXIMUM INITIAL LATERAL WEB DEFORMATION

Calling w_i the lateral web deflection at any point of the cross section of the test panels, shown in Fig. 23, the moment can be expressed as:

$$\frac{d^2 w_i}{dy^2} = \frac{M_i}{EI} \qquad \text{Considering only the absolute value} \qquad \text{(A-1)}$$

which can be approximated by finite difference as:

$$\frac{w_{(i+1)} - 2w_i + w_{(i-1)}}{(\Delta y)^2} = \frac{M_i}{EI}$$

and since

$$\sigma_{bi} = M_i \frac{c}{I}$$

$$\sigma_{bi} = EI \frac{w_{(i+1)} - 2w_i + w_{(i-1)}}{(\Delta y)^2} \frac{c}{I}$$

where σ_{bi} = secondary bending stress at point "i"

$c = t/2$

and I = moment of inertia of a finite element strip along x-axis (see Fig. 23) so

$$\sigma_{bi} = \frac{Et}{2} \frac{w_{(i+1)} - 2w_i + w_{(i-1)}}{(\Delta y)^2} \qquad (A-2)$$

Assuming no flange rotation, the conditions to be satisfied for point i at the juncture of the flange and web are:

$$w_i = 0 \qquad (A-3)$$

and

$$w_{(i+1)} = w_{(i-1)} \qquad (A-4)$$

Thus, the secondary bending stresses at that juncture can be expressed as:

$$\sigma_b = \frac{Et}{(\Delta y)^2} w_{(i+1)} \qquad (A-5)$$

defining

$$w_{(i+1)} = \delta_{(i+1)} - \delta_{o(i+1)}$$

= net web movement

where

$\delta_{o(i+1)}$ = initial lateral eccentricity at point (i+1)

$\delta_{(i+1)}$ = the total lateral measured movement at point (i+1) from the theoretical x-y plane at P_{max}

If $\delta_{(i+1)} = K \delta_{o(i+1)}$, then

$$w_{(i+1)} = (K-1) \delta_{o(i+1)} \qquad (A-6)$$

Considering that the amplification of the maximum initial web eccentricity is larger at the compression side, the web portion of the effective cross section suggested in Reference 4, will be used (Fig.23b).

A column condition will be approximated for this web portion, assuming a force P uniformly distributed in the resulting t x 30t cross sectional area. The critical buckling load of the same web segment is called P'_{cr}.

The solution is based on the assumption that the initial deflected shape follows a sine curve with pinned end conditions. From Reference 7:

$$\delta = \frac{\delta_o}{1 - \lambda} \sin \frac{\pi x}{a} \tag{A-7}$$

where

$$\lambda = P/P'_{cr}$$

$$\delta_o = \text{Maximum initial web deflection.} \tag{A-8}$$

so

$$K = \frac{\delta}{\delta_o} = \frac{1}{1 - \lambda} \tag{A-9}$$

When the portion of the web under consideration has yielded then

$$P = \sigma_{yw}(30t^2) \tag{A-10}$$

and

$$P'_{cr} = \frac{\pi^2 EI_y}{a^2} = \frac{5\pi^2 Et^4}{2a^2} \tag{A-11}$$

thus

$$\lambda = \frac{12}{\pi^2} \frac{\sigma_{yw}}{E} (a/t)^2 \tag{A-12}$$

Substituting into equation (A-5) values from equations (A-6) and (A-9) σ_b becomes:

$$\sigma_b = \frac{Et}{(\Delta y)^2} \left[\frac{1}{1 - \lambda} - 1 \right] \delta_o \qquad \text{(A-13)}$$

or

$$\delta_o = \frac{\sigma_b (\Delta y)^2}{Et} \left[\frac{1}{\lambda} - 1 \right] \qquad \text{(A-14)}$$

and by substituting to this equation the value of λ from (A-12):

$$\frac{\delta_o}{t} = \frac{\sigma_b (\Delta y)^2}{Et^2} \left[\frac{\pi^2}{12} \frac{E}{\sigma_{yw}} (t/a)^2 - 1 \right] \qquad \text{(A-15)}$$

It has been concluded in section 4.2 that type 1 cracks will not develop if σ_b is less than the yield stress σ_{yw} of the web. Therefore, cracking will be avoided if

$$\frac{\delta_o}{t} \leq \frac{\sigma_{yw} (\Delta y)^2}{Et^2} \left[\frac{\pi^2}{12} \frac{E}{\sigma_{yw}} (t/a)^2 - 1 \right] \qquad \text{(A-16)}$$

The first term in the bracket of equation (A-16) is negligible because of the ratio (t/a), which is very small

$$\frac{\delta_o}{t} \leq \frac{\sigma_{yw} (\Delta y)^2}{Et^2} \qquad \text{(A-17)}$$

Consequently, to fit the experimental data it is assumed that $\Delta_y \approx 30t$. Thus, equation (A-17) becomes

$$\frac{\delta_o}{t} \leq \frac{\sigma_{yw} (30t)^2}{Et^2} \qquad \text{(A-18)}$$

or

$$\frac{\delta_o}{t} \leq \text{approx. } 1000 \frac{\sigma_{yw}}{E} \qquad \text{(A-19)}$$

REFERENCES

1. Lew, H. S., and Toprac, A. A., "Fatigue Test of Hybrid Plate Girders under Constant Moment," Research Report No. 77-2F, report to the Texas Highway Department, C. F. H. R. The University of Texas, January 1967.

2. ASTM Committee E-9, "A Guide for Fatigue Testing and the Statistical Analysis of Fatigue Data," Special Technical Publication No. 91-A (1963).

3. AASHO, "Standard Specifications for Highway Bridges," Ninth Edition. Washington, D. C., 1965.

4. Basler, K. and Thürlimann, B., "Strength of Plate Girders," Fritz Laboratory Reprint #210, Lehigh University.

5. Yen, B. T. and Mueller, J. A., "Fatigue Test of Large-Size Welded Plate Girders," Fritz Laboratory Report No. 303.10, Lehigh University (1966).

6. Lew, H. S., and Toprac, A. A., "Fatigue Strength of Hybrid Plate Girders under Constant Moment," Highway Research Record No. 167. Highway Research Board. 1967.

7. Timoshenko, S. P., and Gere, J. M., "Theory of Elastic Stability," 2nd Edition, McGraw-Hill Book Company, Inc.

8. Zienkiewicz, O. C., and Holister, G. S., "Stress Analysis," 1st Edition. John Wiley & Sons Ltd., 1965.

9. Fielding, D. J., "Fatigue Tests of Slender-Web Hybrid Plate Girders under Combined Moment and Shear," Master thesis, The University of Texas, 1968.

10. Richmond, S. B., "Statistical Analysis," 2nd Edition, The Ronald Press Co., 1964.

11. Wilson, A., "Stepwise Regression," Fortran Program written from the BIMED statistical Programs of U. C. L. A., 1966.

TABLE 1

SUMMARY OF PREVIOUS FATIGUE TEST RESULTS*

Specimen	β**	Cycles to Initial Crack	Type of Crack
21020A	295	2,927,000	No Crack
21530A	295	2,000,000	No Crack
21540A	295	294,000	1
22540A	295	1,318,700	3c
		1,722,400	1
22550A	295	617,800	1,2
21020B	269	2,233,000	No Crack
21530B	269	2,137,300	No Crack
21540B	269	277,400	Testing Discontinued
22540B	269	1,588,000	1
22550B	269	672,000	1
31020B	190	4,770,900	No Crack
31530B	190	2,104,360	No Crack
31540B	190	890,000	2
		919,000	2
		1,132,100	2
32540B	190	2,440,000	No Crack
32550B	190	815,300	1
		911,530	3b
41020A	141	2,311,200	No Crack
41530A	141	2,000,000	No Crack
41540A	141	630,000	3a
42540A	141	947,200	3c
42550A	141	639,500	3c
41530B	147	2,052,800	No Crack
41540B	147	974,000	2
		974,000	2
42540B	147	3,643,000	No Crack
42550B	147	421,000	2
61530A	93	2,000,000	No Crack
61540A	93	1,394,800	2,3a
62540A	93	2,530,000	No Crack
62550A	93	479,000	3b

*From Reference 1

**Based on measured dimensions

TABLE 2

MECHANICAL AND CHEMICAL PROPERTIES

			Flange (1/2")	Web (3/16")	Web (10 gage)
Material Properties	σ_y (ksi)	Tested	111.08	51.68	32.18
		Reported	113.30	-----	-----
	σ_u (ksi)	Tested	123.45	62.15	47.79
		Reported	123.80	64.40	-----
Chemical Components		C	0.20	0.10	Not Reported
		Mn	0.62	0.44	
		P	0.01	0.01	
		S	0.018	0.024	
		Cu	0.27	0.22	
		Si	0.35	0.06	
		Mo	0.24	-----	
		Ti	0.082	-----	
		Cr	1.08	-----	
		B	0.002	-----	

TABLE 3

CROSS SECTION DIMENSIONS

Specimen	Measured Dimensions		β Ratio
	Flange	Web	(Measured)
22050D	8" x 0.512"	36" x 0.135"	267
22050DR	8" x 0.504"	36" x 0.135"	267
32050D	7.98" x 0.512"	36" x 0.183"	197
32050DR	7.48" x 0.511"	36" x 0.183"	197

TABLE 4

REFERENCE LOADS

Girder	σ_{cr} (red.)	P_{cr}	P_y	P_{max}	P_{min}	$\frac{P_{max}}{P_{cr}}$	$\frac{P_{min}}{P_{cr}}$
22050D*	76.5	130.9	60.7	89.4	34.4	0.68	0.26
22050DR*	77.0	129.8	59.8	88.1	33.9	0.68	0.26
32050D*	98.5	170.6	102.7	96.6	38.6	0.57	0.23
32050DR**	95.9	158.1	97.5	91.7	36.7	0.58	0.23

*8" flange width.

**7 1/2" flange width.

TABLE 5 - SUMMARY OF TEST RESULTS

GIRDER	WEB THICK.	CRACK LOCATIONS (NEAR SIDE)	CRACK NO.	FIRST OBSERVED AT CYCLES	FIRST OBSERVED AT SIDE	IN BOTH SIDES AT (CYCLES)	TYPE	REMARKS
22050D	10 ga.	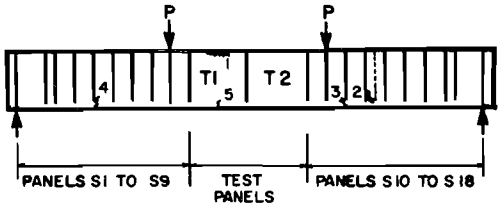	1	230,000	N.S	257,000	1	
			2	450,000	BOTH	450,000	2	
			CRACK NO. 2 REPAIRED AT 456,000 CYCLES. STIFFNER (SHOWN IN DASHED LINE) ADDED					
			3	544,000	BOTH	544,000	2	
			4	544,000	BOTH	544,000	2	
			5	544,000	BOTH	544,000	3	PENETRATED FL.
22050DR	10 ga.	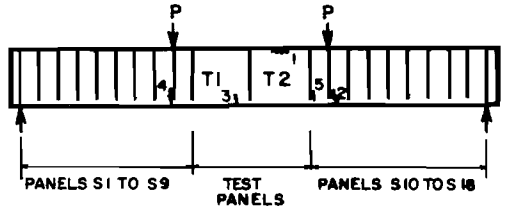	1	532,000	BOTH	532,000	1	
			2	546,000	F.S.	591,000	2	
			3	560,000	F.S.	591,000	3	
			4	609,000	N.S	-	2	N.S. ONLY
			5	615,000	F.S.	-	2	F.S. ONLY
32050D	3/16"	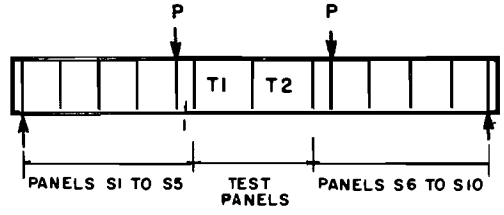	1	496,000	F.S.	-	3	F.S. ONLY
			CRACK NO. 1 REPAIRED AT 496,000 CYCLES					
			1	566,000	BOTH	566,000	3	REAPPEARED. PENETRATED INTO FLANGE
32050DR	3/16"	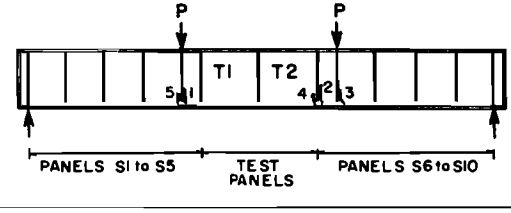	1	439,000	N.S.	487,000	2	
			2	527,000	N.S.	-	2	N.S. ONLY
			3	527,000	BOTH	527,000	2	
			CRACKS NO. 1, 2 & 3 REPAIRED AT 527,000 CYCLES					
			4	560,000	N.S.	-	2	N.S. ONLY
			5	560,000	N.S.	-	2	N.S. ONLY

NOTES:

A.- ALL GIRDERS SHOWN IN THEIR NEAR SIDE (POSITIVE Z)

B.- DETAILS OF CRACKS IN FIGS. 12, 13, 14 & 15.

C.- N.S. = NEAR SIDE
F.S. = FAR SIDE

TABLE 6.- MULTIPLE REGRESSION ANALYSIS DATA

SPECIMEN	NUMBER OF CYCLES (10^3 CYCLES) TO				$\left(\frac{\delta_o}{t}\right)_{max}$	$\left(\frac{\delta_{oc}}{t}\right)_{max}$	$\sigma_{min.}$ (ksi)	$\sigma_{max.}$ (ksi)	σ_R (ksi)	β	$\frac{\sigma_{max.}}{\sigma_{cr}}$
	1st CRACK	TYPE 1	TYPE 2	TYPE 3							
21020 A	2,927 *				1.61	1.61	10.0	20.0	10.0	295.0	0.32
21530 A	2,000 *				1.55	1.55	15.0	30.0	15.0		0.47
21540 A	294	294			1.69	1.69	15.0	40.0	25.0		0.63
22540 A	1,318.7	1,722.4		1,318.7	1.62	1.62	25.0	40.0	15.0		0.61
22550 A	617.8	617.8	617.8		2.09	2.09	25.0	50.0	25.0		0.78
21020 B	2,233 *				1.72	1.72	10.0	20.0	10.0	269.0	0.27
21530 B	2,137.3 *				0.71	0.36	15.0	30.0	15.0		0.40
22540 B	1,588	1,588			1.35	1.11	25.0	40.0	15.0		0.53
22550 B	672	672			1.51	1.32	25.0	50.0	25.0		0.67
31020 B	4,700.9 *				0.89	0.69	10.0	20.0	10.0	190.0	0.21
31530 B	2,104.4 *				0.99	0.99	15.0	30.0	15.0		0.32
31540 B	890		890		1.39	0.92	15.0	40.0	25.0		0.43
	919		919		0.56	0.38	15.0	40.0	25.0		0.43
32540 B	2,440 *				0.87	0.87	25.0	40.0	15.0		0.43
32550 B	911.5			911.5	1.41	1.03	25.0	50.0	25.0		0.53
	815.3	815.3			1.45	0.88	25.0	50.0	25.0		0.53
41020 A	2,311.2 *				0.24	0.20	10.0	20.0	10.0	141.0	0.21
41530 A	2,000 *				0.15	0.15	15.0	30.0	15.0		0.32
41540 A	630			630	0.29	0.29	15.0	40.0	25.0		0.42
42540 A	947.2			947.2	0.21	0.21	25.0	40.0	15.0		0.42
42550 A	639.5			639.5	0.14	0.13	25.0	50.0	25.0		0.53
41530 B	2,052.8*				0.17	0.16	15.0	30.0	15.0	147.0	0.32
41540 B	974.0		974		0.48	0.48	15.0	40.0	25.0		0.43
	974.0		974		0.36	0.36	15.0	40.0	25.0		0.43
42540 B	3,643.0 *				0.52	0.52	25.0	40.0	15.0		0.43
42550 B	421.0		421.0		0.57	0.57	25.0	50.0	25.0		0.53
61530 A	2,000.0*				0.24	0.24	15.0	30.0	15.0	93.0	0.32
61540 A	1,394.8		1,394.8	1,394.8	0.35	0.24	15.0	40.0	25.0		0.42
62540 A	2,530.0*				0.34	0.34	25.0	40.0	15.0		0.42
62550 A	479.0			479.0	0.22	0.22	25.0	50.0	25.0		0.53
22050 D	230.0	230.0		544	1.89	0.76	20.0	50.0	30.0	267.0	0.65
22050 DR	546.0			546.0	1.68	1.52	20.0	50.0	30.0		0.65
	532.0	532.0			1.74	1.29	20.0	50.0	30.0		0.65
32050 D	566.0			566.0	0.66	0.57	20.0	50.0	30.0	197.0	0.51
32050 DR	439.0		439.0		0.82	0.42	20.0	50.0	30.0		0.52
	527.0		527.0		1.37	1.19	20.0	50.0	30.0		0.52

* RUN — OUT SPECIMENS. N = $2,000 \times 10^3$ cycles FOR THE REGRESSION

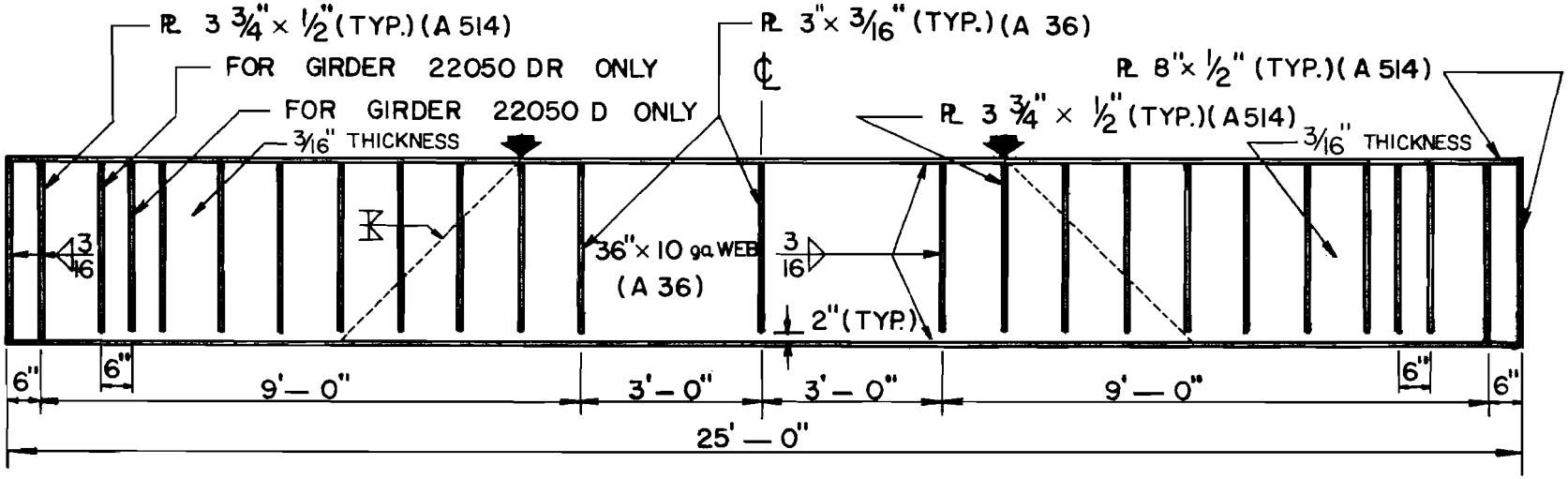

a) GIRDERS 22050 D AND 22050 DR

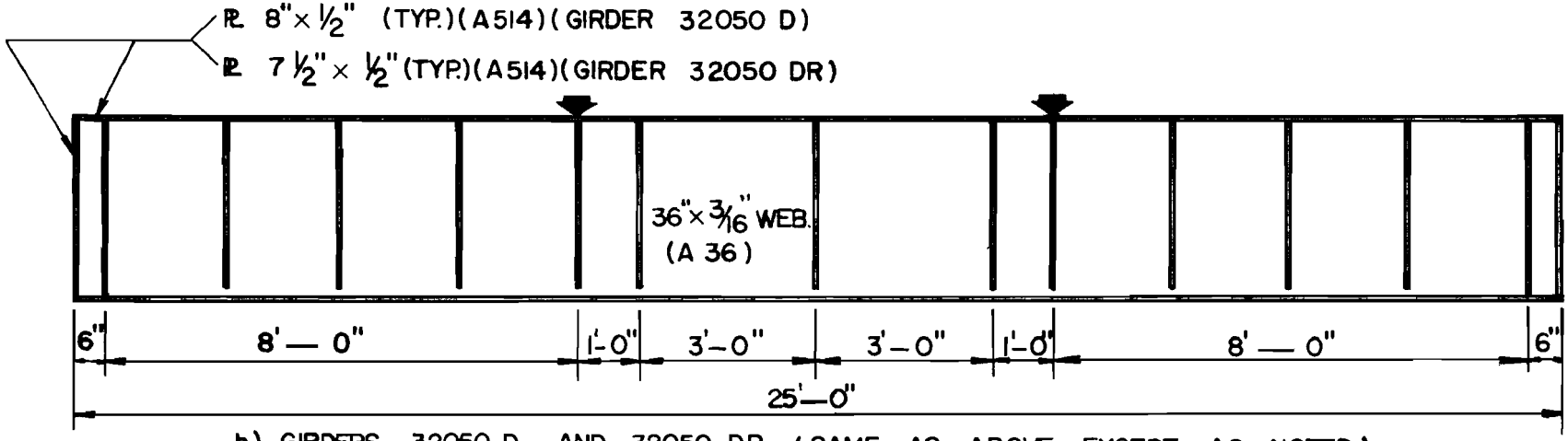

b) GIRDERS 32050 D AND 32050 DR (SAME AS ABOVE EXCEPT AS NOTED)

FIG. 1 SPECIMEN DIMENSIONS AND DETAILS

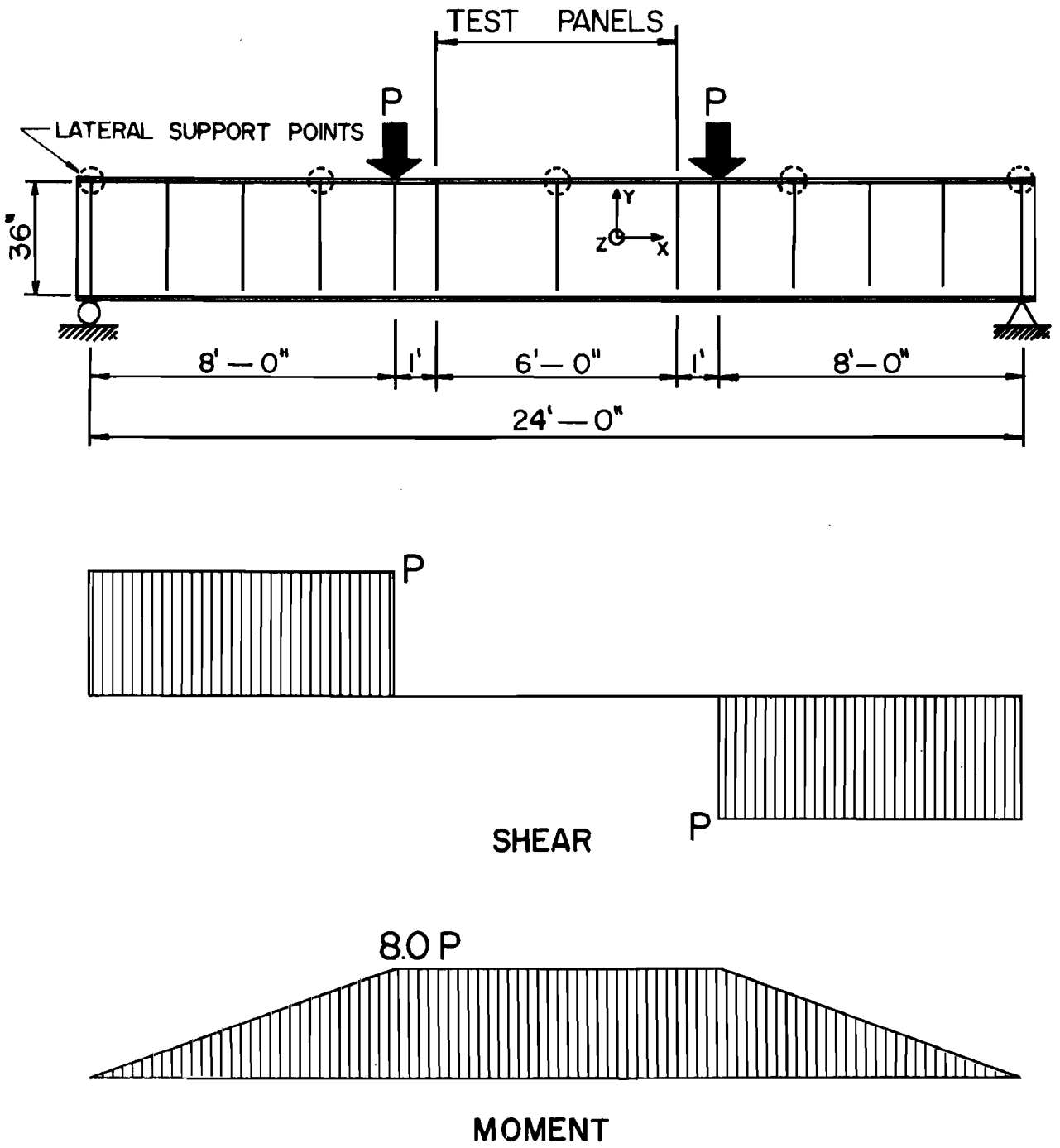

FIG. 2 TEST SETUP

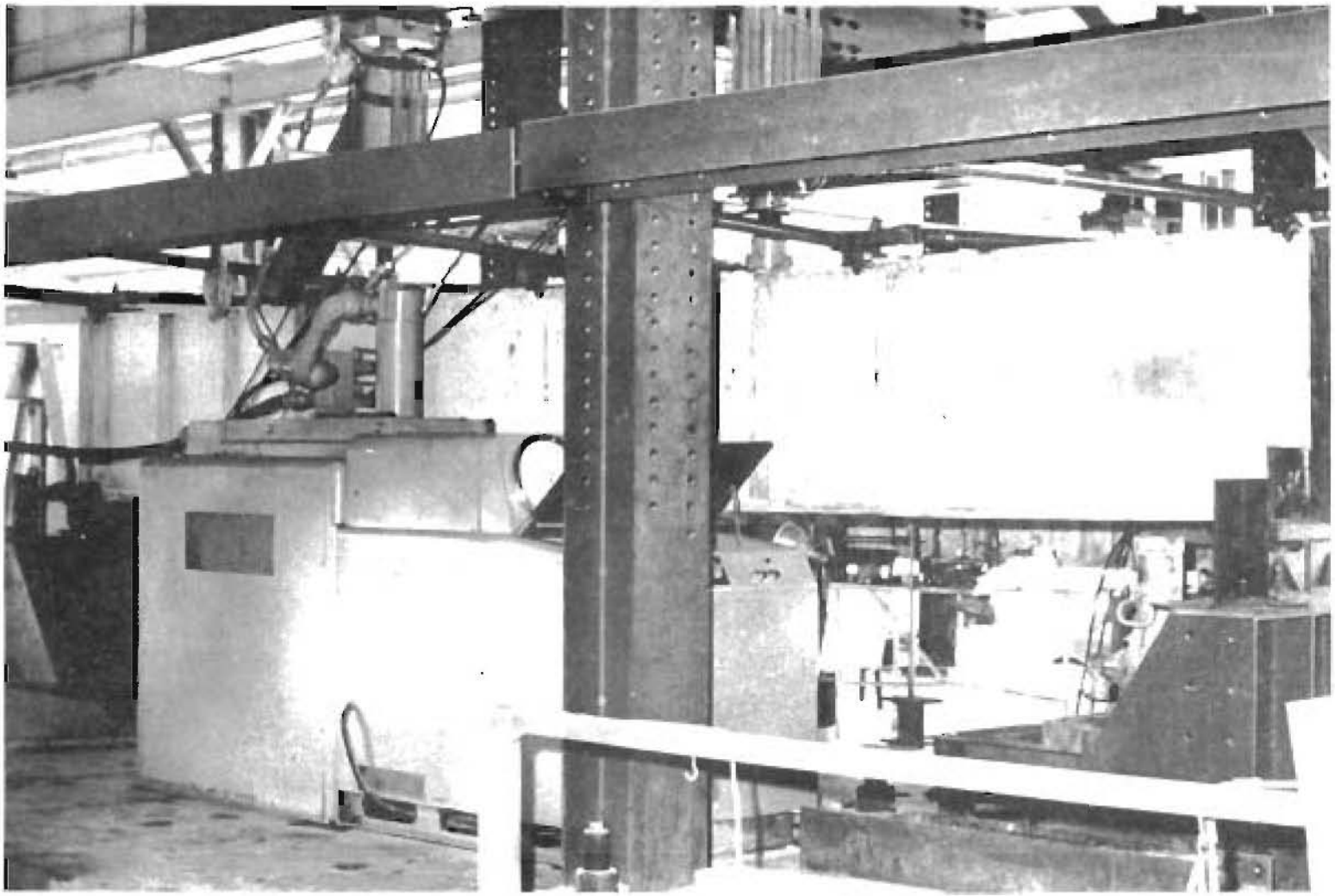

FIG. 3 OVERALL VIEW OF TEST SETUP

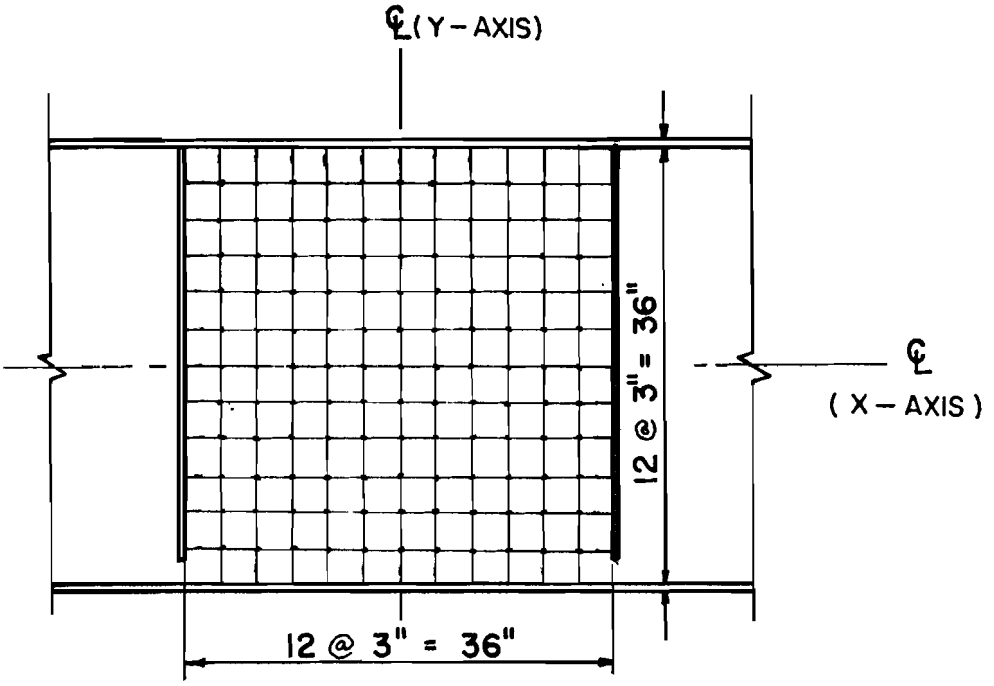

FIG 4 LOCATIONS OF LATERAL WEB DEFLECTION MEASUREMENT

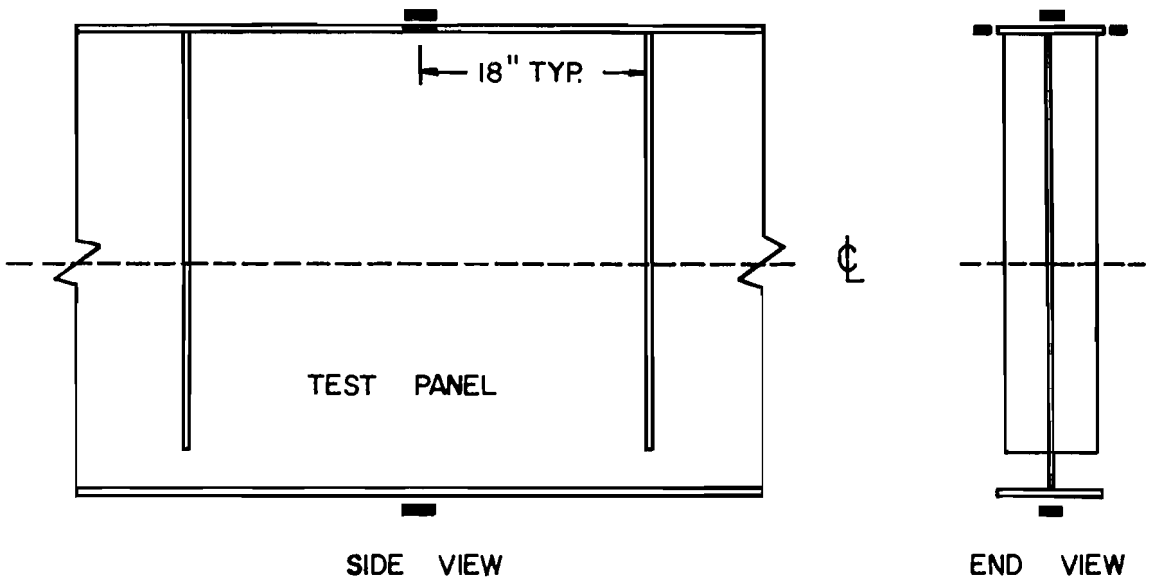

ALL GAGES ARE SR4 – A5 – S6

FIG. 5 TYPICAL STRAIN GAGE LOCATIONS

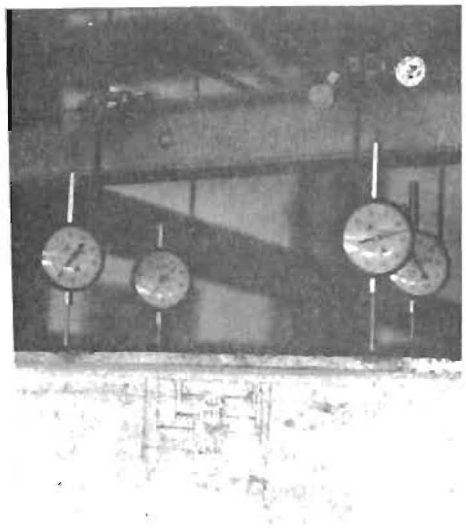

FIG. 6 MEASUREMENT OF FLANGE ROTATION

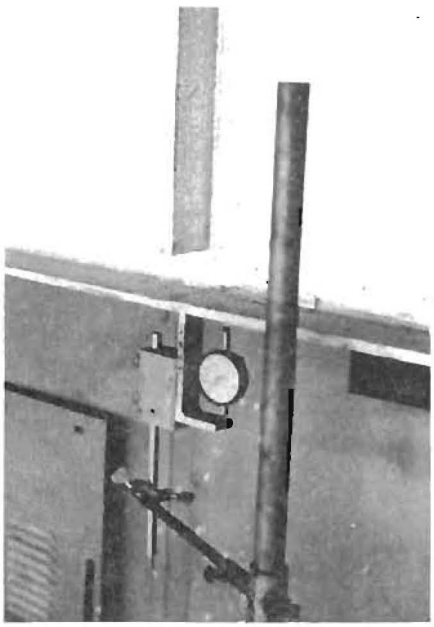

FIG. 7 SLIP GAGE

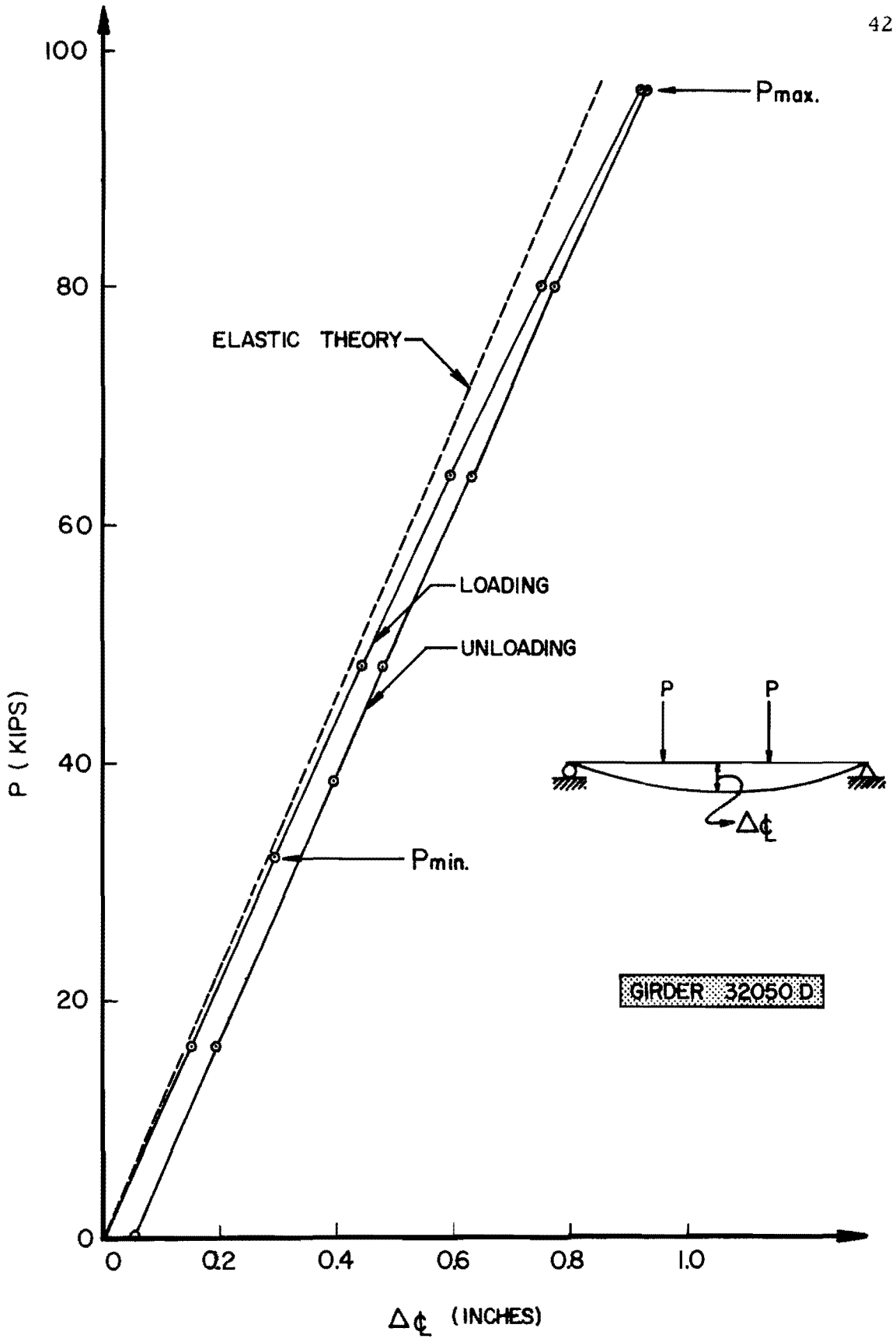

FIG. 8 LOAD vs DEFLECTION CURVE FOR GIRDER 32050 D

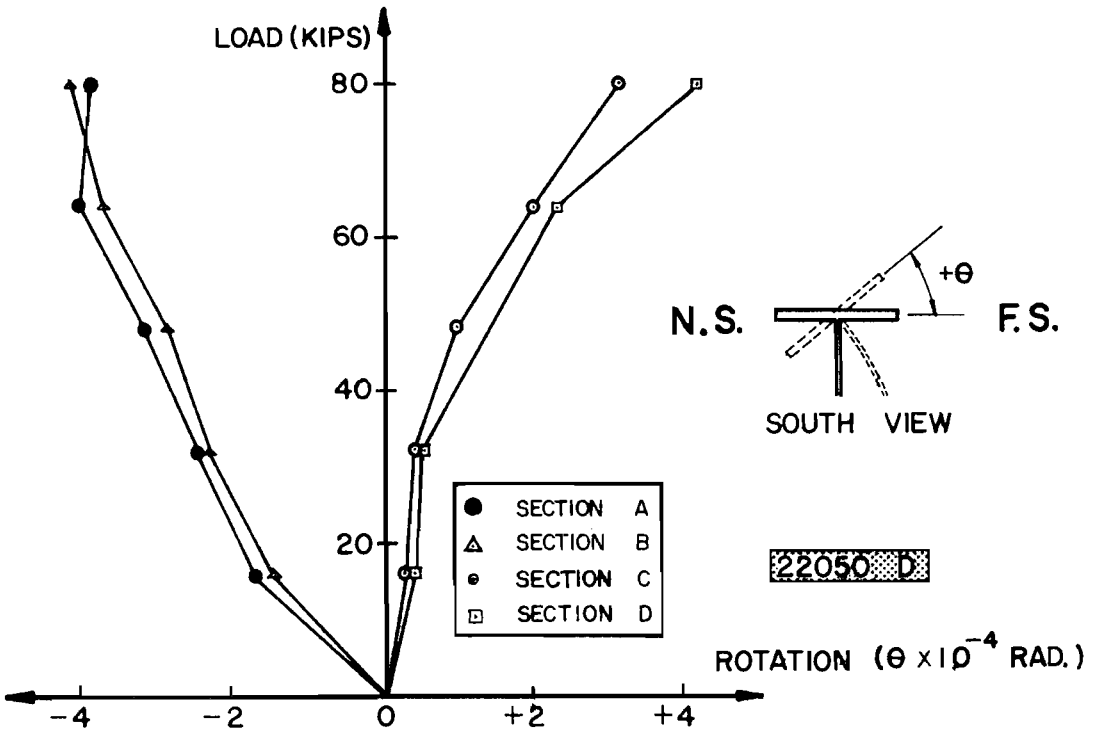

a) OPPOSITE DIRECTION ROTATIONS

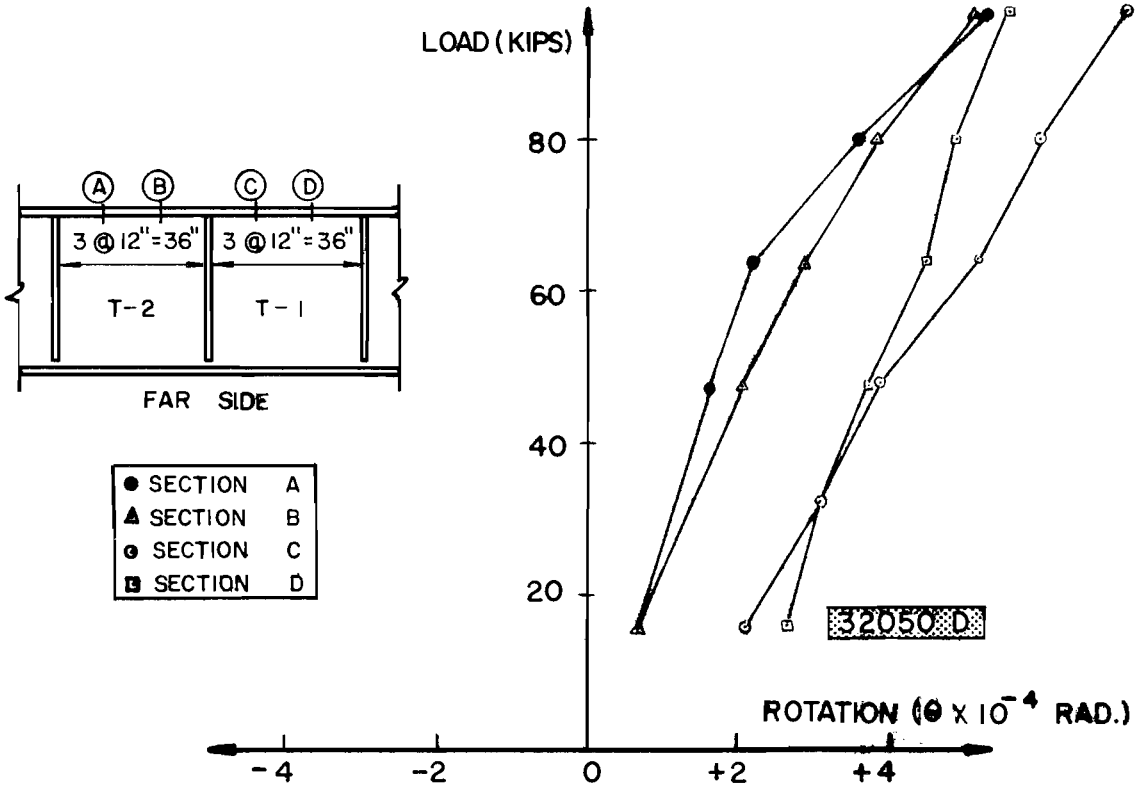

b) SAME DIRECTION ROTATIONS

FIG. 9 TYPICAL LOAD vs ROTATION CURVES

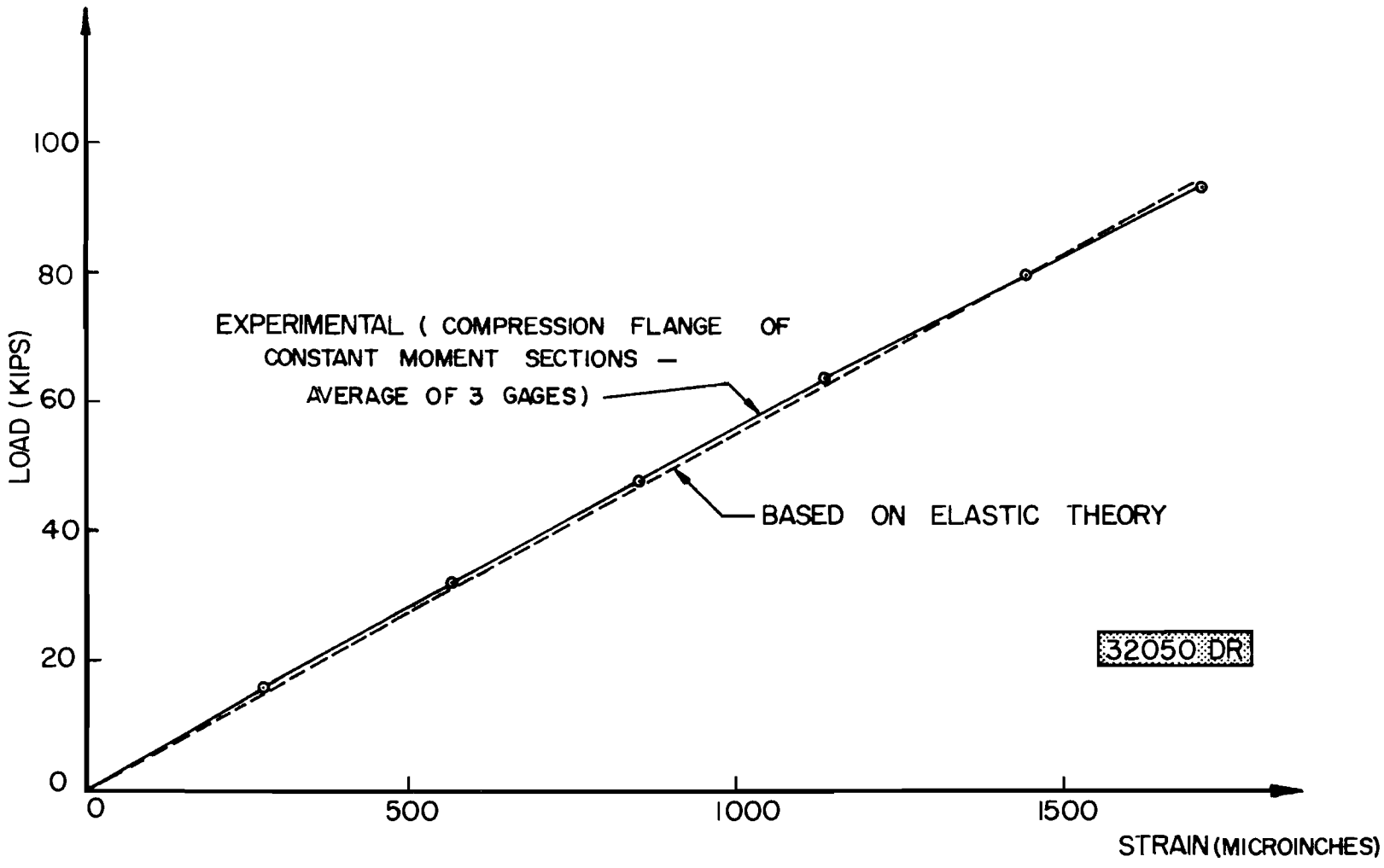

FIG. 10 TYPICAL LOAD vs STRAIN CURVE

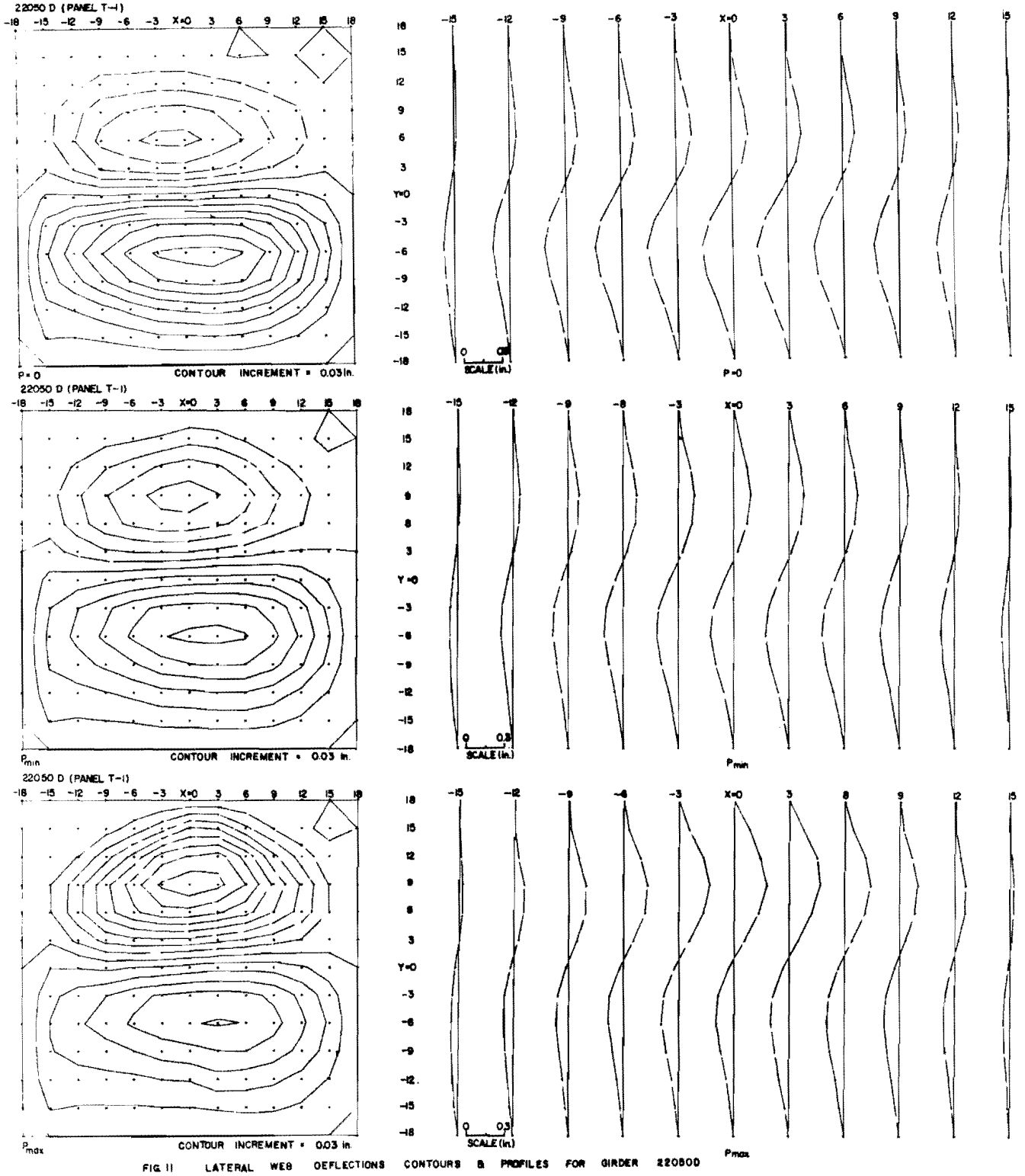

FIG. 11 LATERAL WEB DEFLECTIONS CONTOURS & PROFILES FOR GIRDER 220500

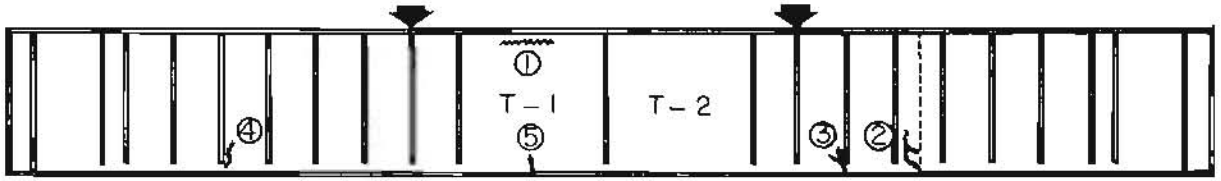

NEAR SIDE

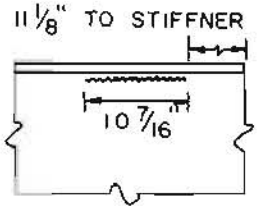

CRACK #1 (N.S.)

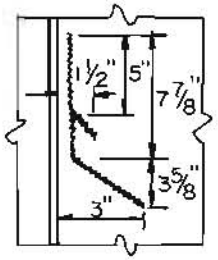

CRACK #2 (N.S.)

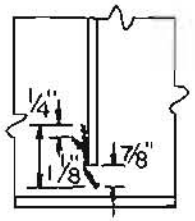

CRACK #3 (N.S.)

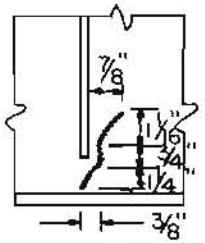

CRACK #4 (N.S.)

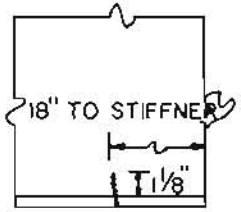

CRACK #5 (N.S.)

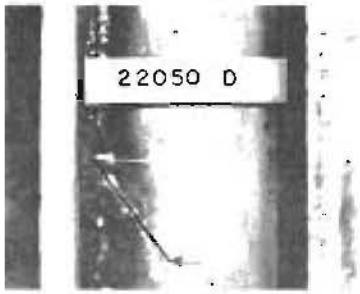

CRACK # 2 (F.S.)

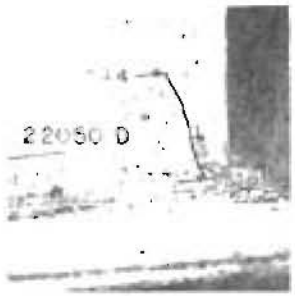

CRACK # 3 (F.S.)

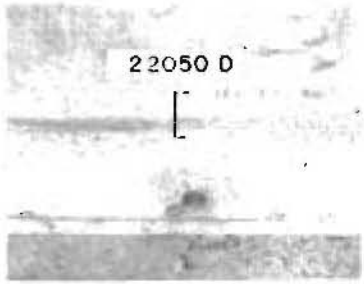

CRACK # 5 (F.S.)

FIG. 12 CRACK DETAILS OF GIRDER 22050 D

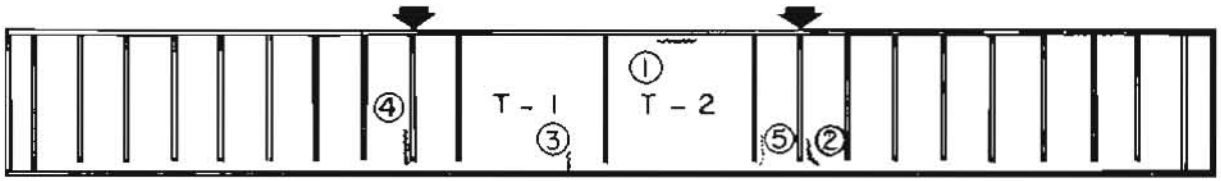

NEAR SIDE

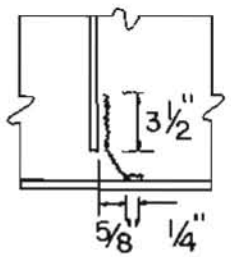

CRACK Nº 2 (N.S)

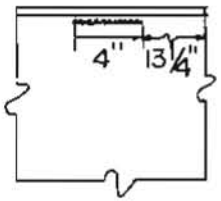

CRACK Nº 1 (N.S)

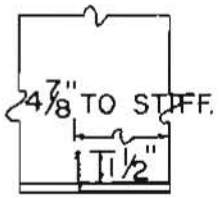

CRACK Nº 3 (N.S)

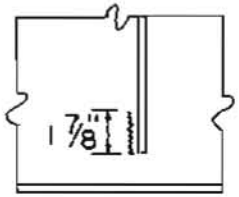

CRACK Nº 4 (N.S)

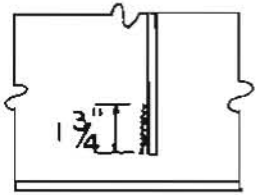

CRACK Nº 5 (F.S)

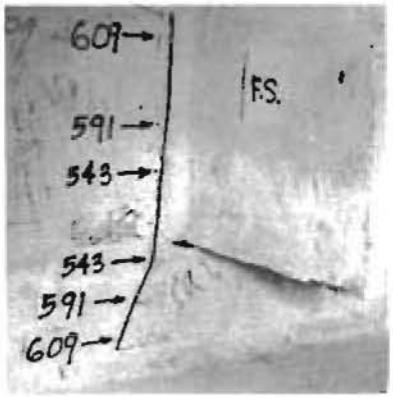

CRACK Nº 2 (F.S)

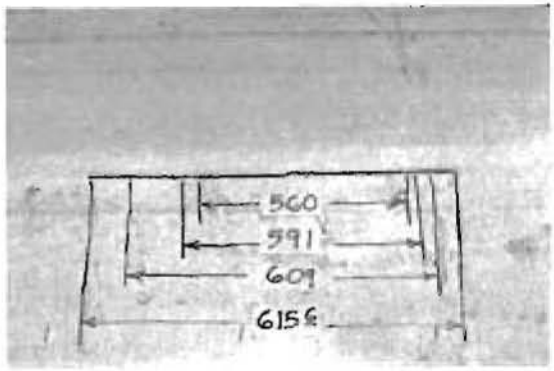

CRACK Nº 1 (F.S)

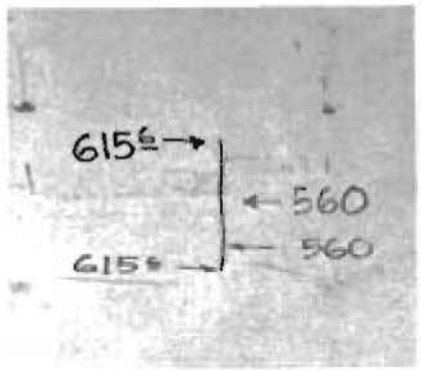

CRACK Nº 3 (F.S)

FIG. 13 CRACK DETAILS OF GIRDER 22050 DR

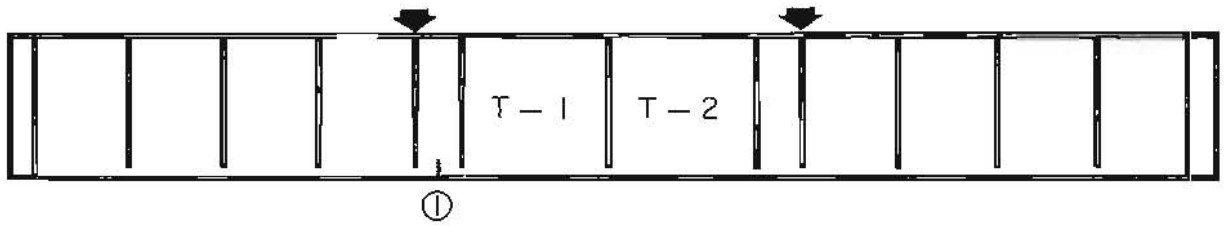

NEAR SIDE

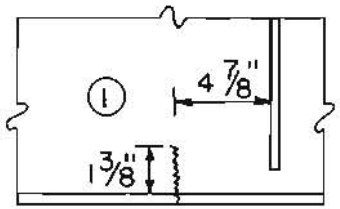

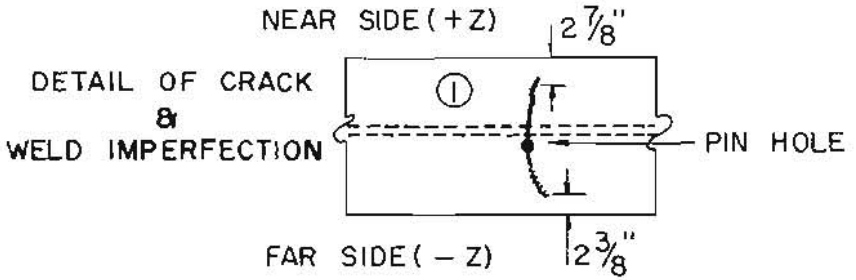

NEAR SIDE VIEW

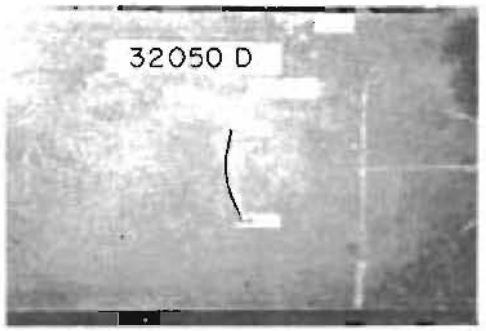

BOTTOM VIEW

FIG. 14 CRACK DETAILS FOR GIRDER 32050 D

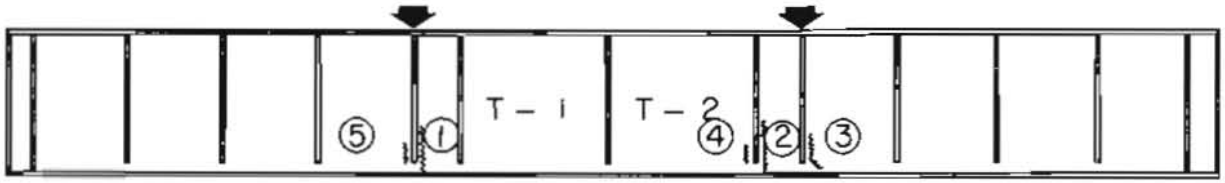

NEAR SIDE

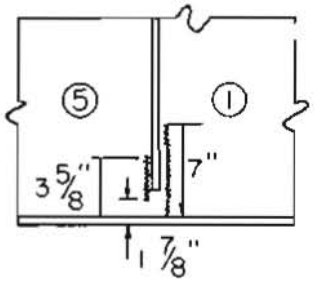

CRACKS Nº 1 AND 5 (N.S.)

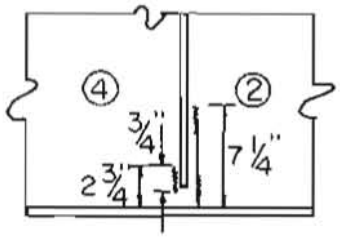

CRACKS Nº 2 AND 4 (N.S)

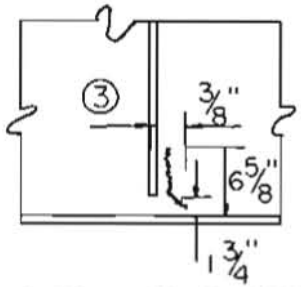

CRACK Nº 3 (N.S.)

OVERALL VIEW OF THE CRACK

FIG. 15 CRACK DETAILS FOR GIRDER 32050 DR

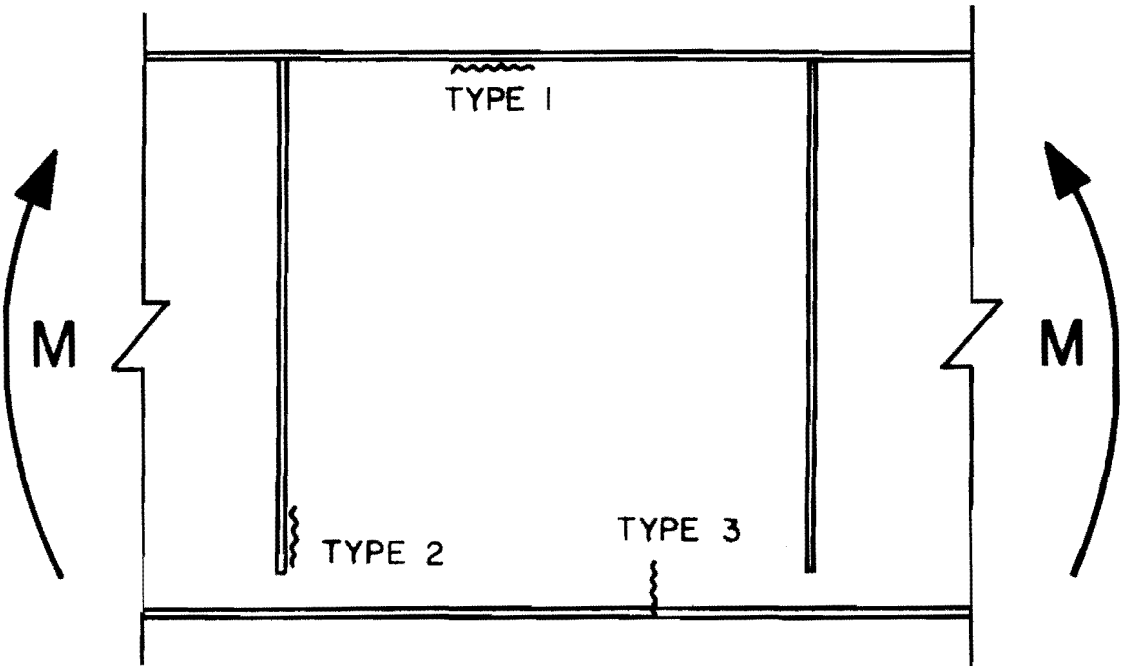

FIG. 16 TYPES OF FATIGUE CRACKS FOR PURE BENDING SPECIMENS

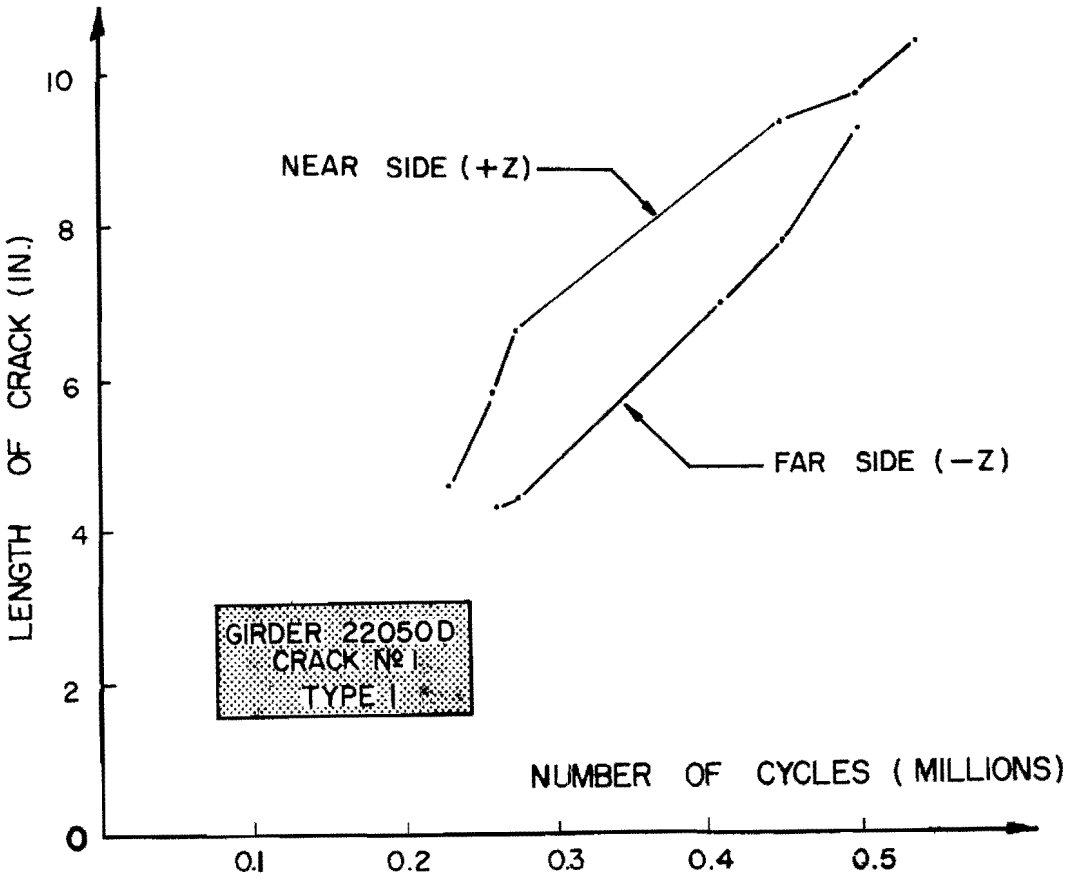

FIG. 17 CRACK PROPAGATION CURVE (TYPE 1 CRACK)

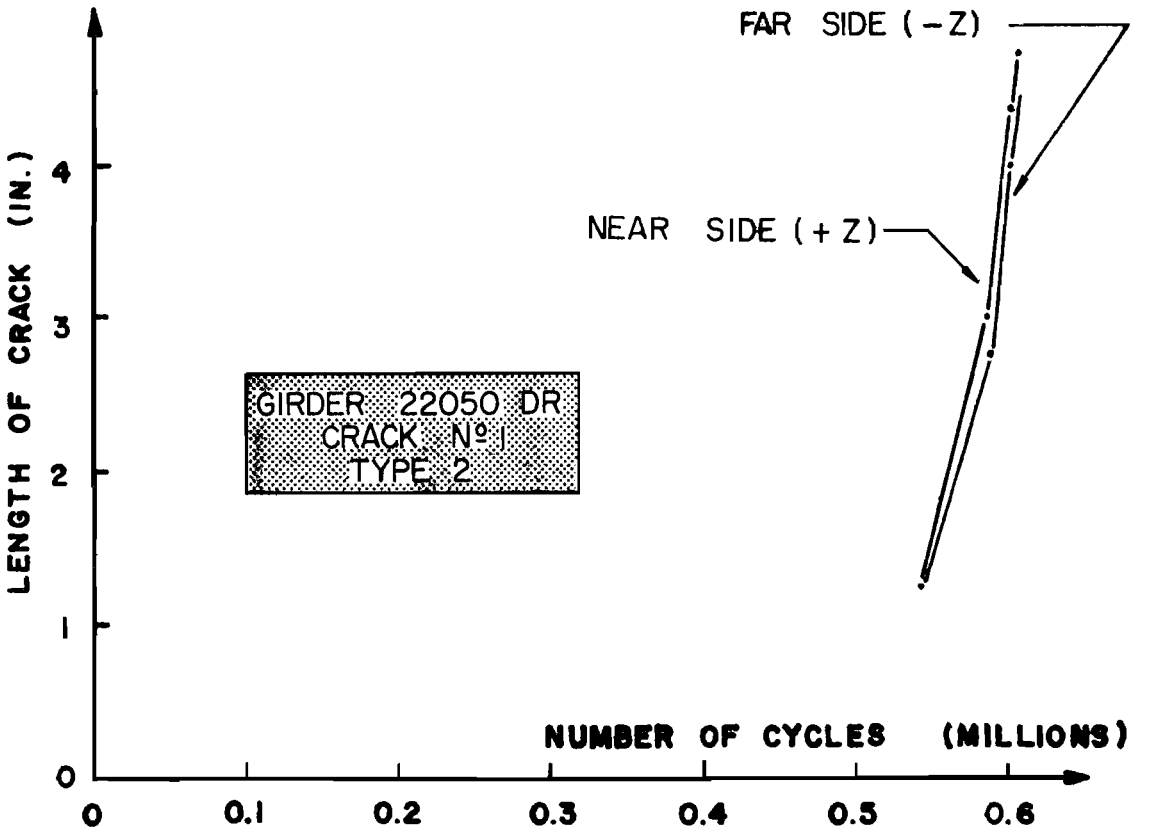

FIG. 18 CRACK PROPAGATION CURVE (TYPE 2 CRACK)

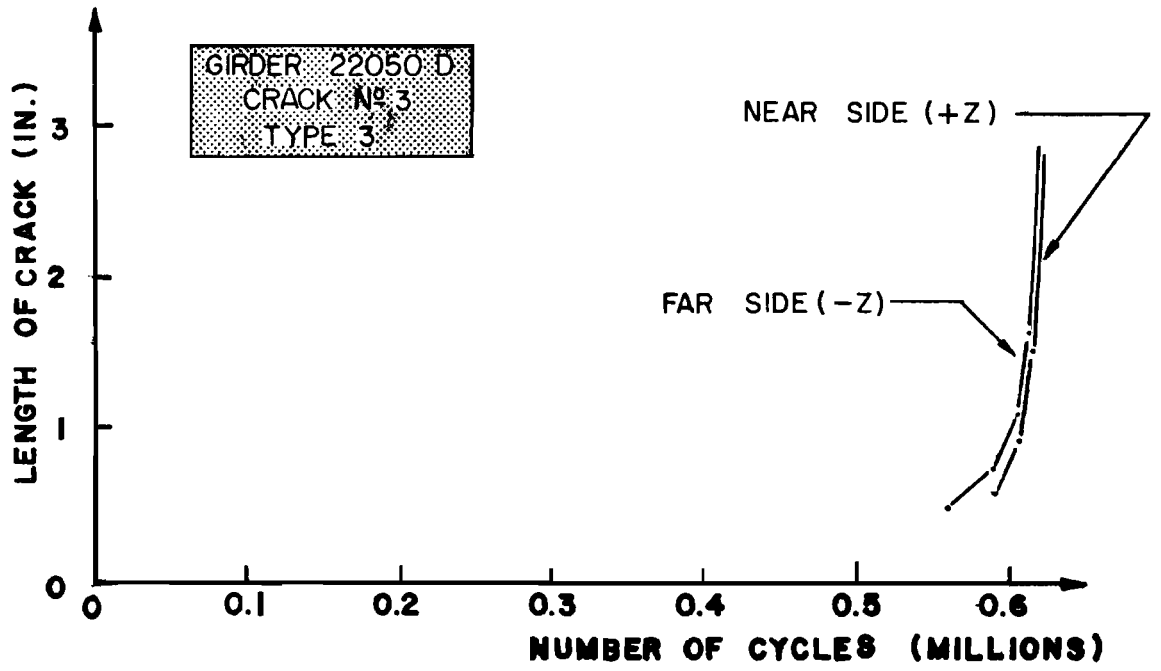

FIG. 19 CRACK PROPAGATION CURVE (TYPE 3 CRACK)

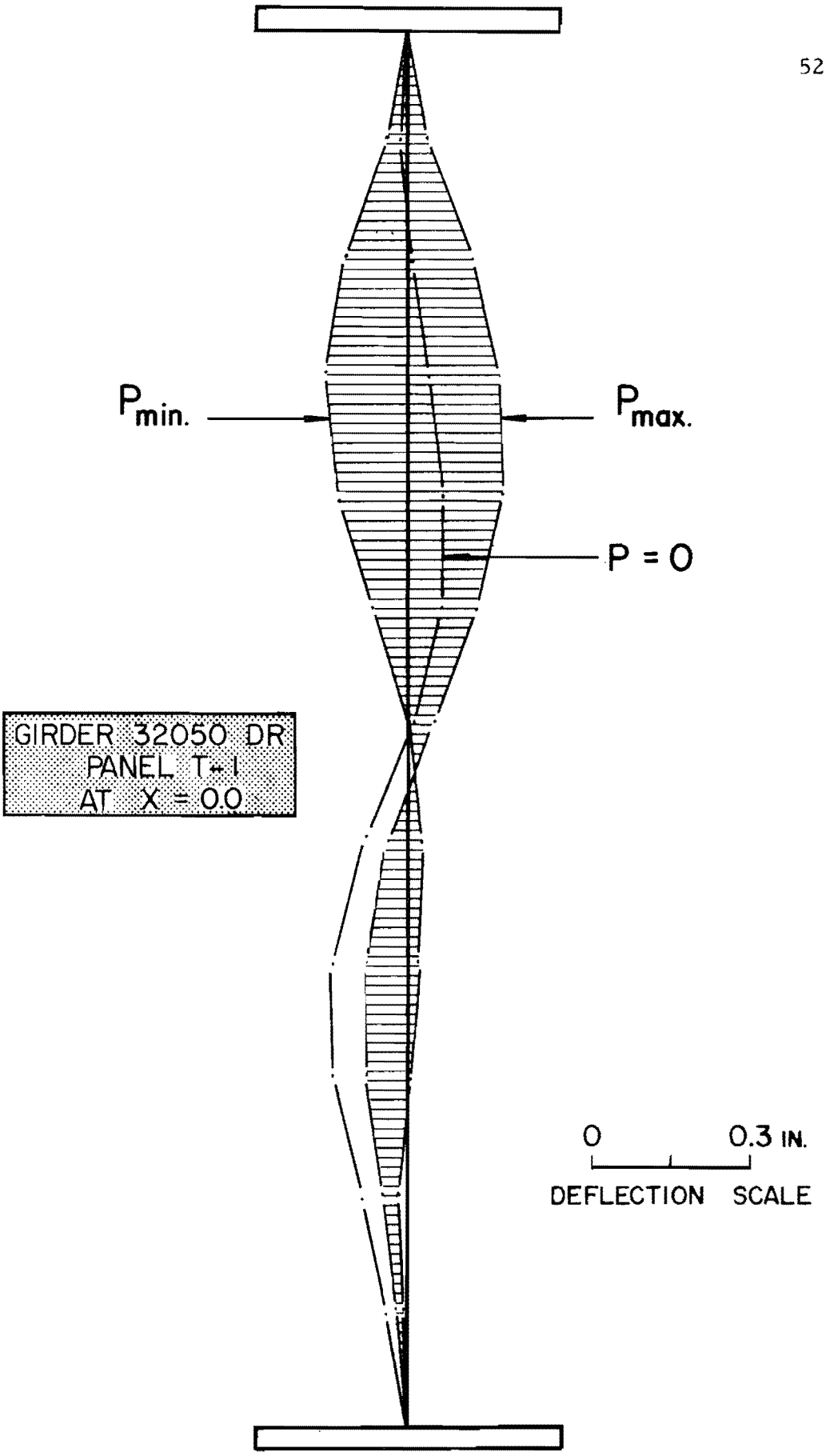

FIG. 20 WEB LATERAL DEFLECTION

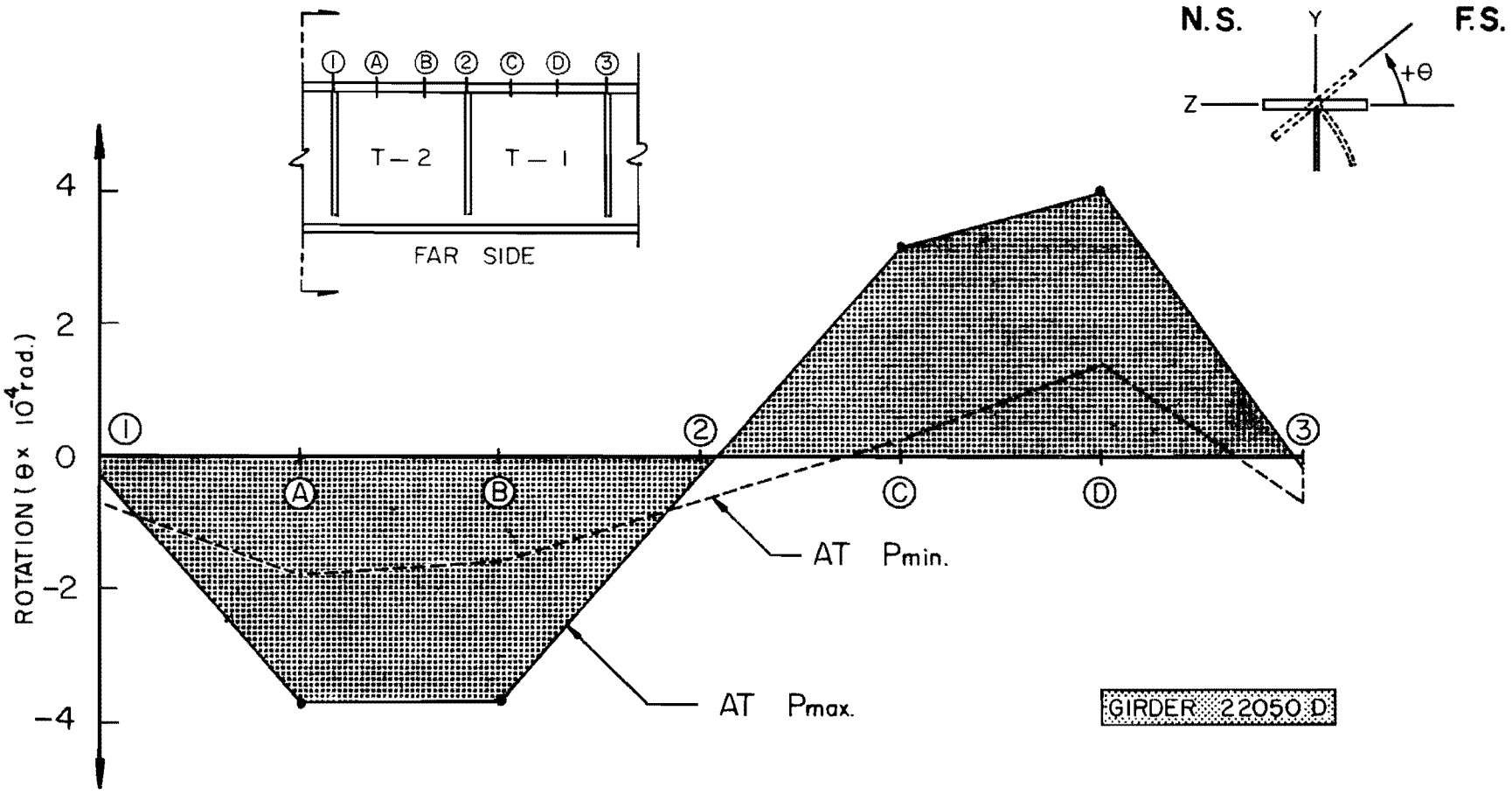

FIG. 21 TYPICAL VARIATION OF FLANGE ROTATIONS

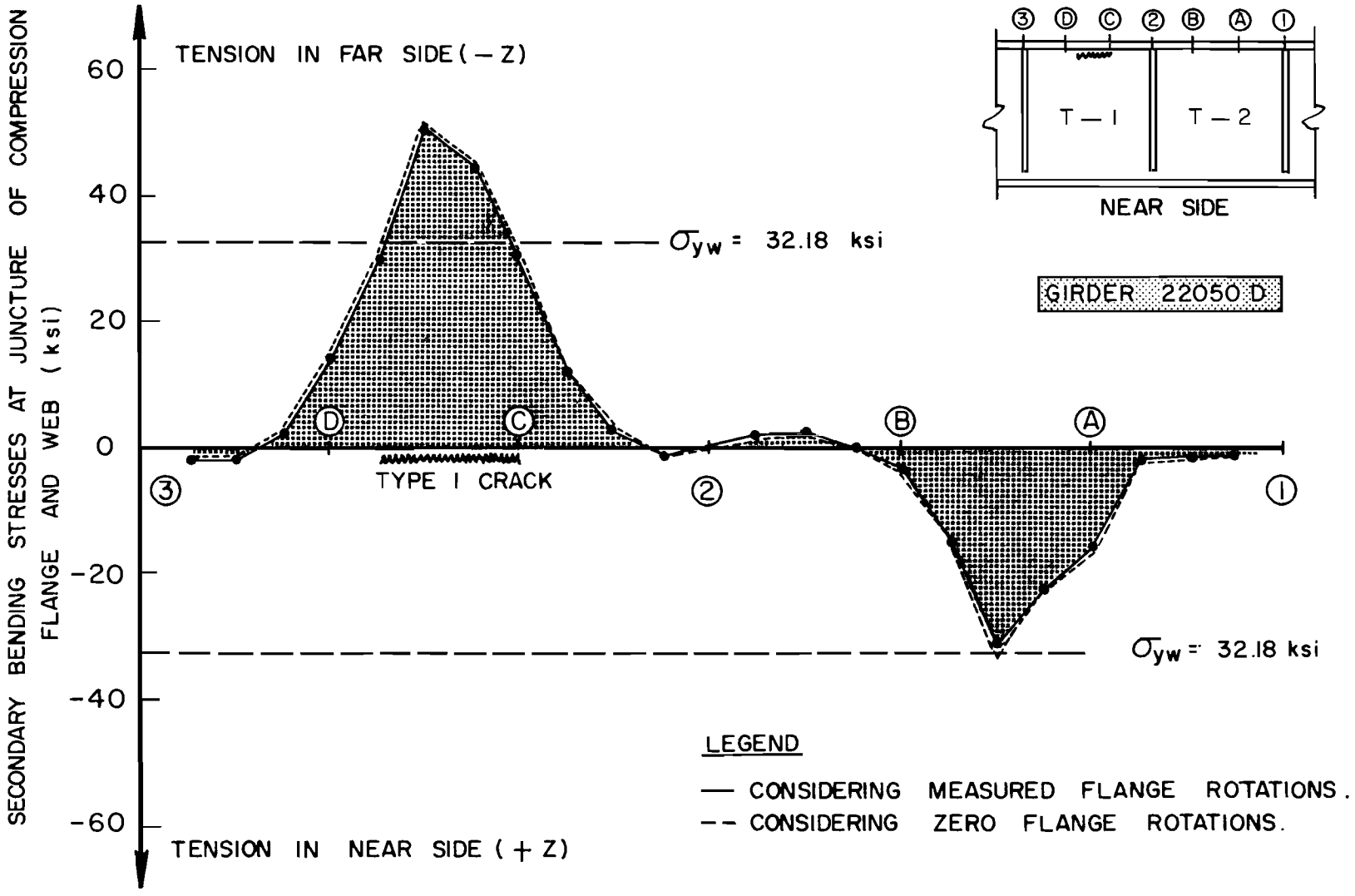

FIG. 22 DISTRIBUTION OF SECONDARY BENDING STRESSES AT Pmax.

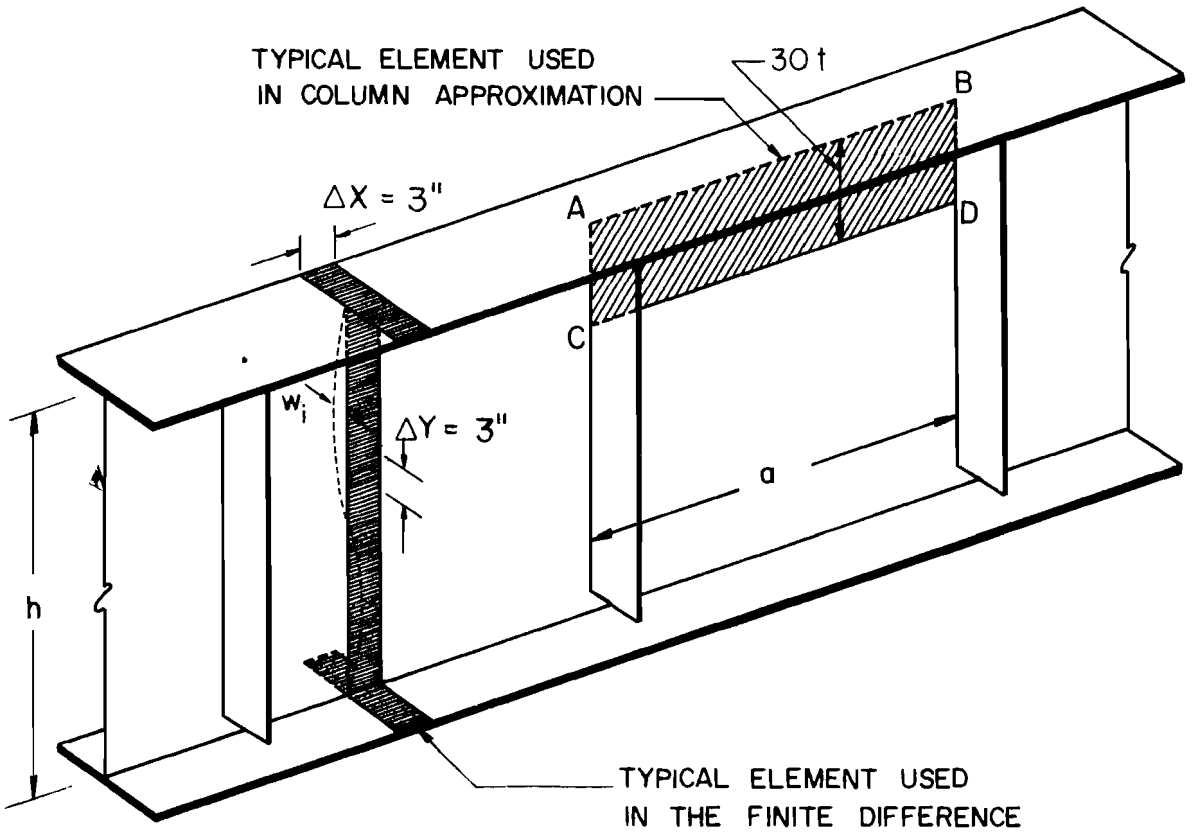

a) TYPICAL ELEMENTS CONSIDERED

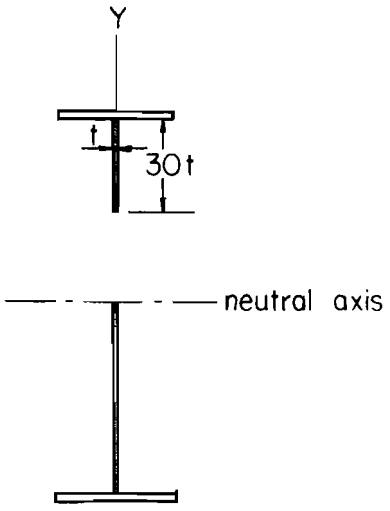

b) EFFECTIVE CROSS SECTION CONSIDERED

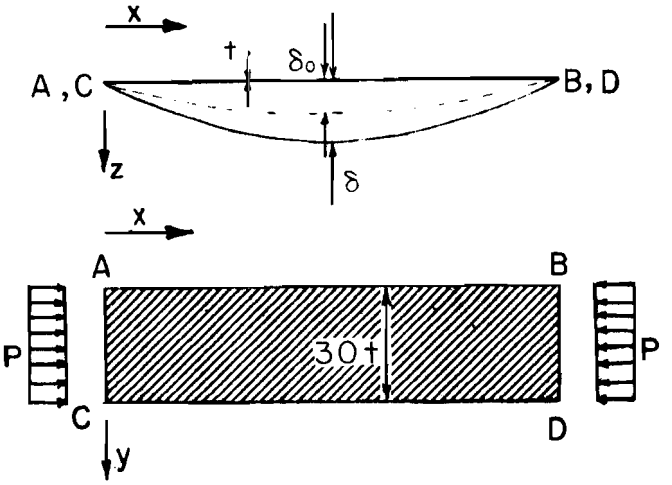

c) COLUMN APPROXIMATION ELEMENT.

FIG. 23 TYPICAL ELEMENTS USED ON THE FINITE DIFFERENCE AND COLUMN APPROXIMATION APPROACH

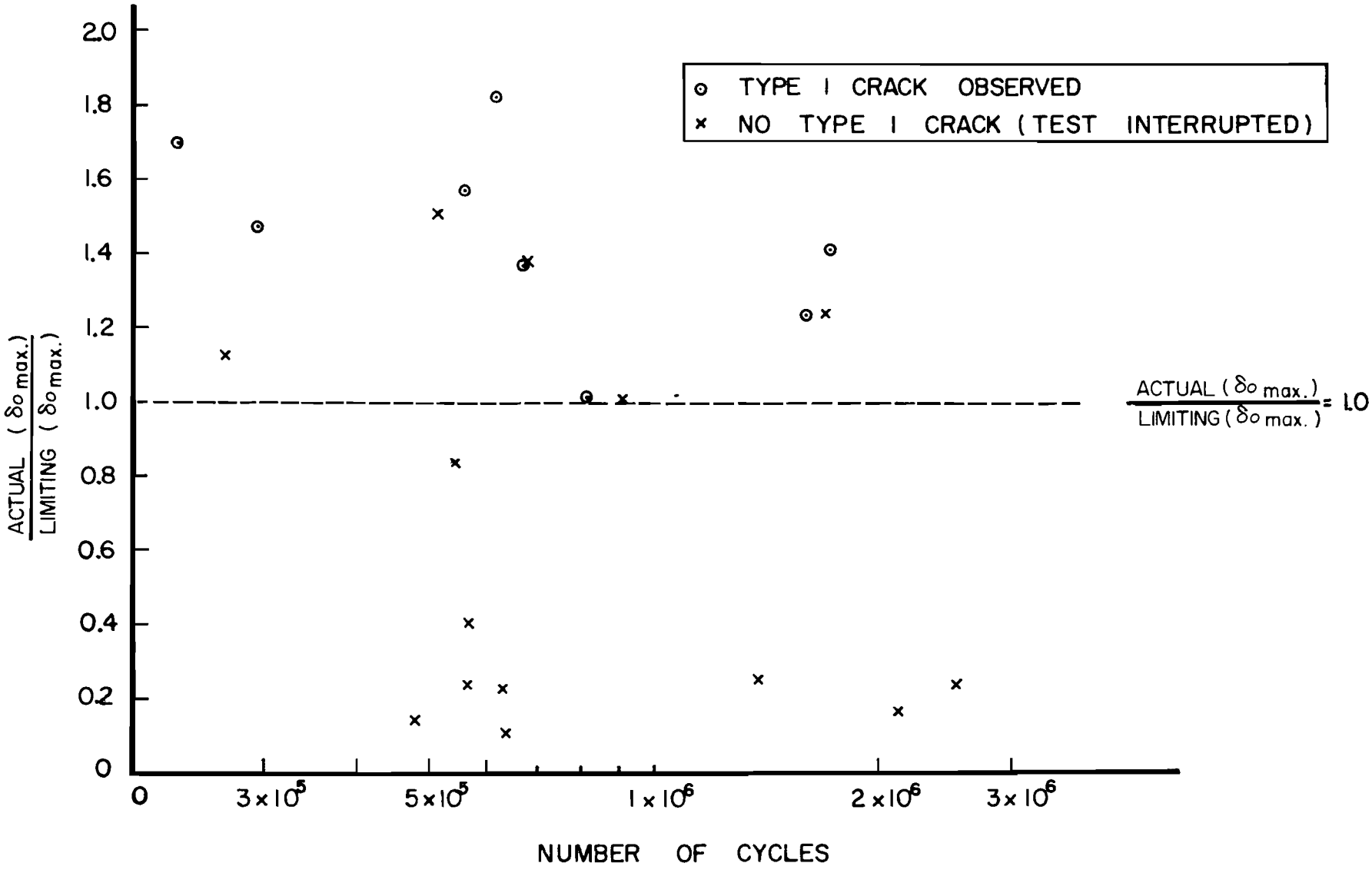

FIG. 24 COMPARISON OF SUGGESTED LIMIT VALUE OF $\left[\frac{\delta o}{t}\right]_{max}$ WITH TEST RESULTS

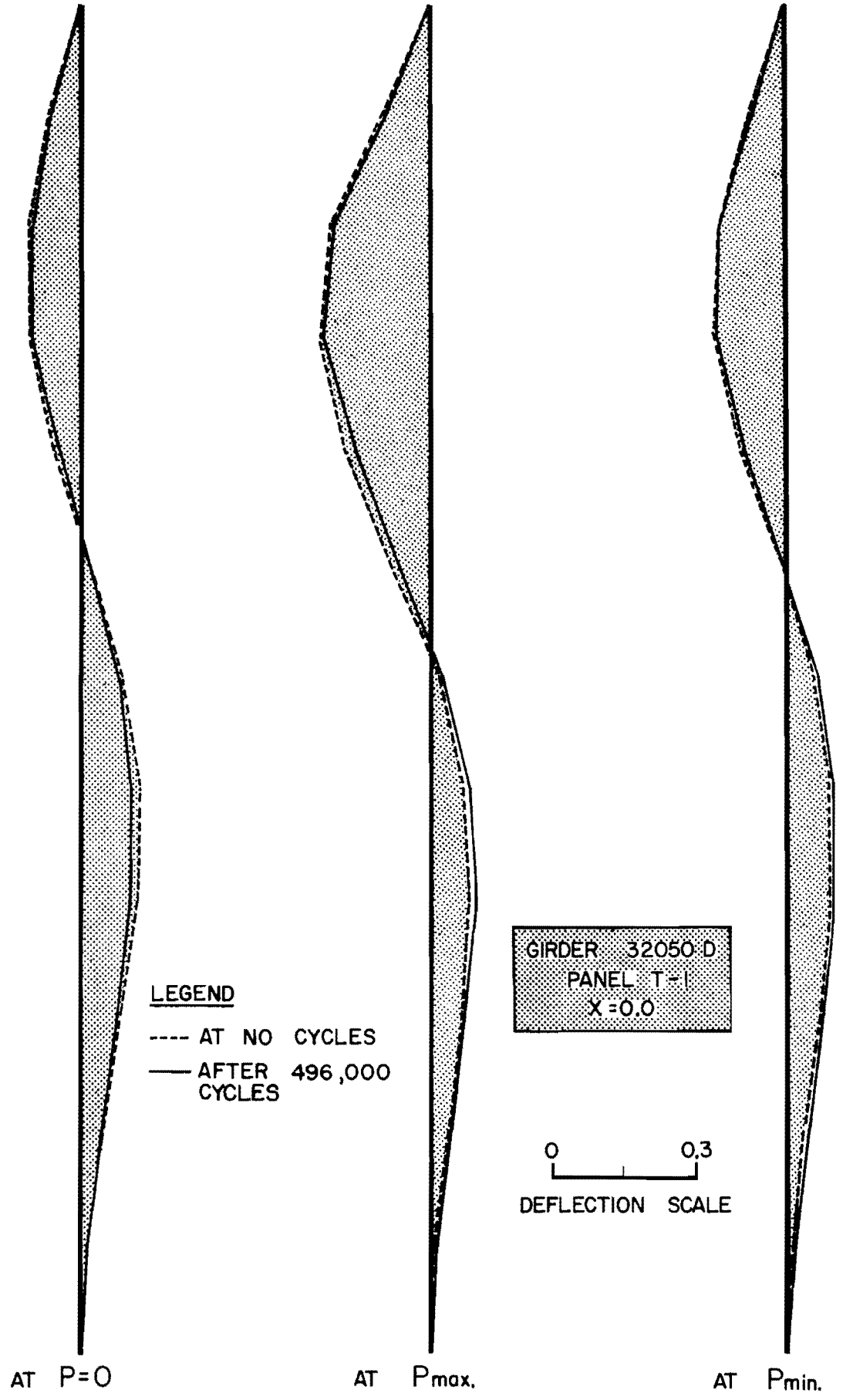

FIG. 25 EFFECT OF FATIGUE CYCLING IN THE LATERAL WEB DEFLECTIONS

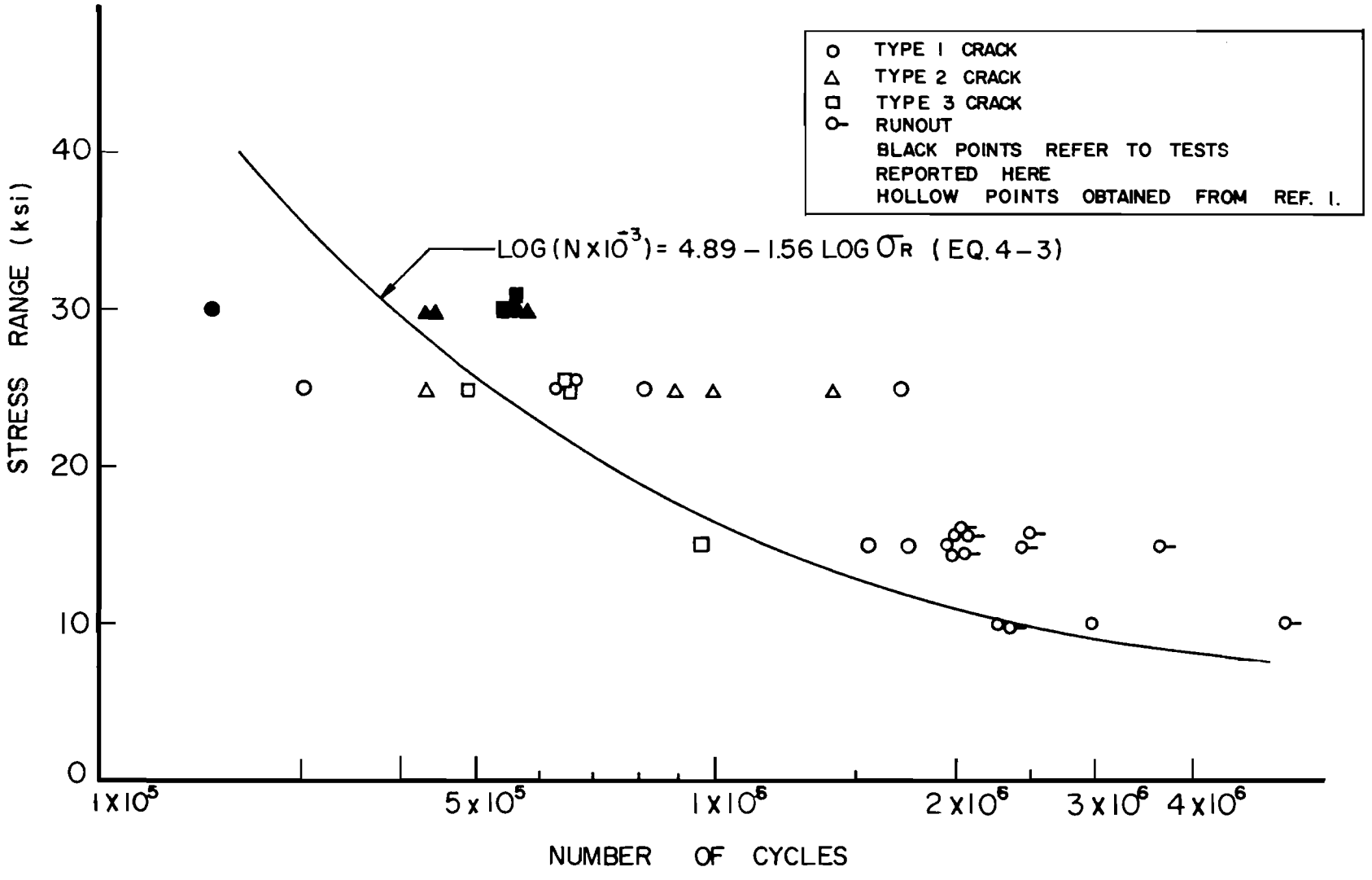

FIG. 26 COMPARISON OF EQ. 4-3 WITH RESULTS

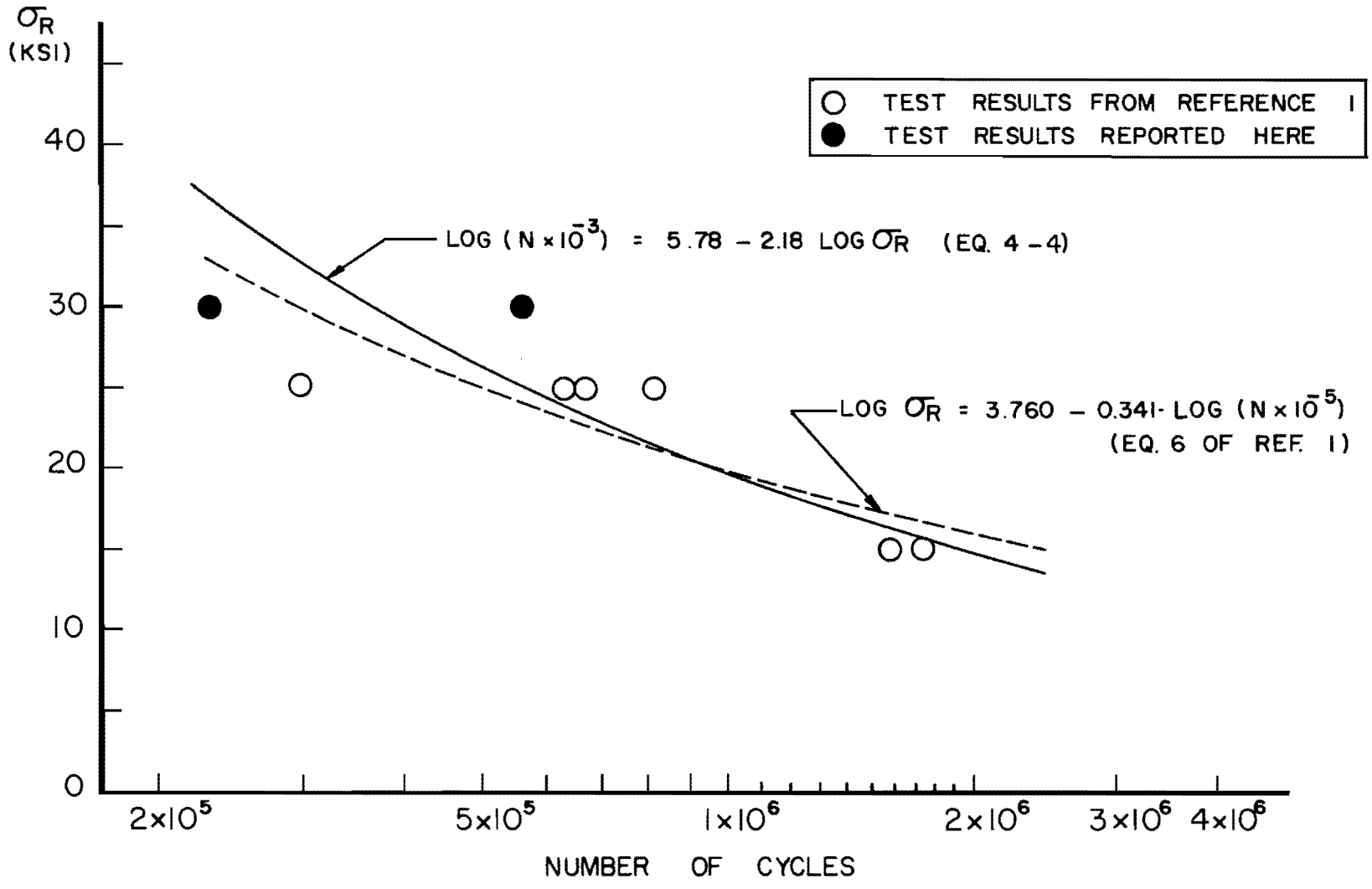

FIG. 27 RESULTS OF TYPE I CRACK

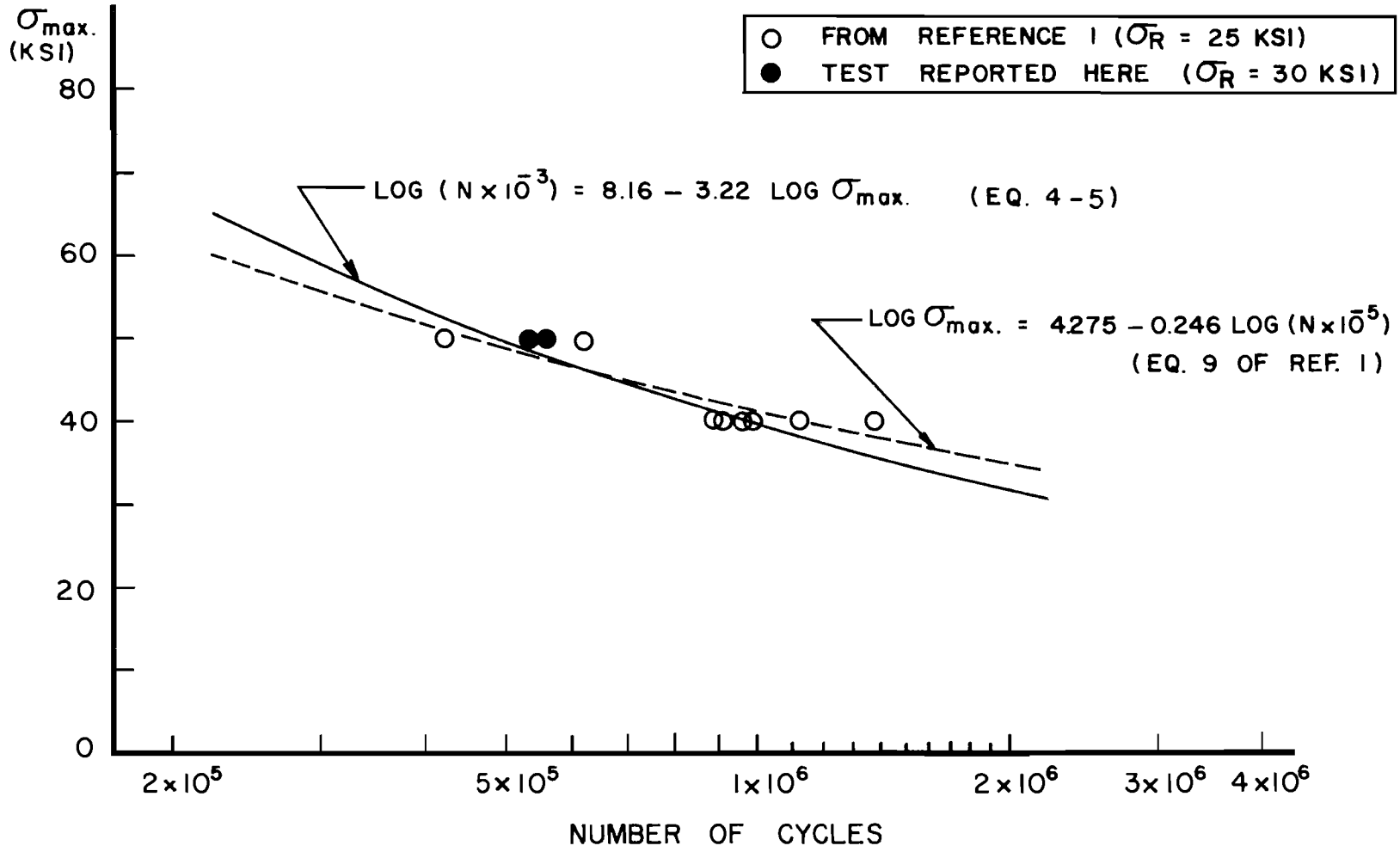

FIG. 28 RESULTS OF TYPE 2 CRACK

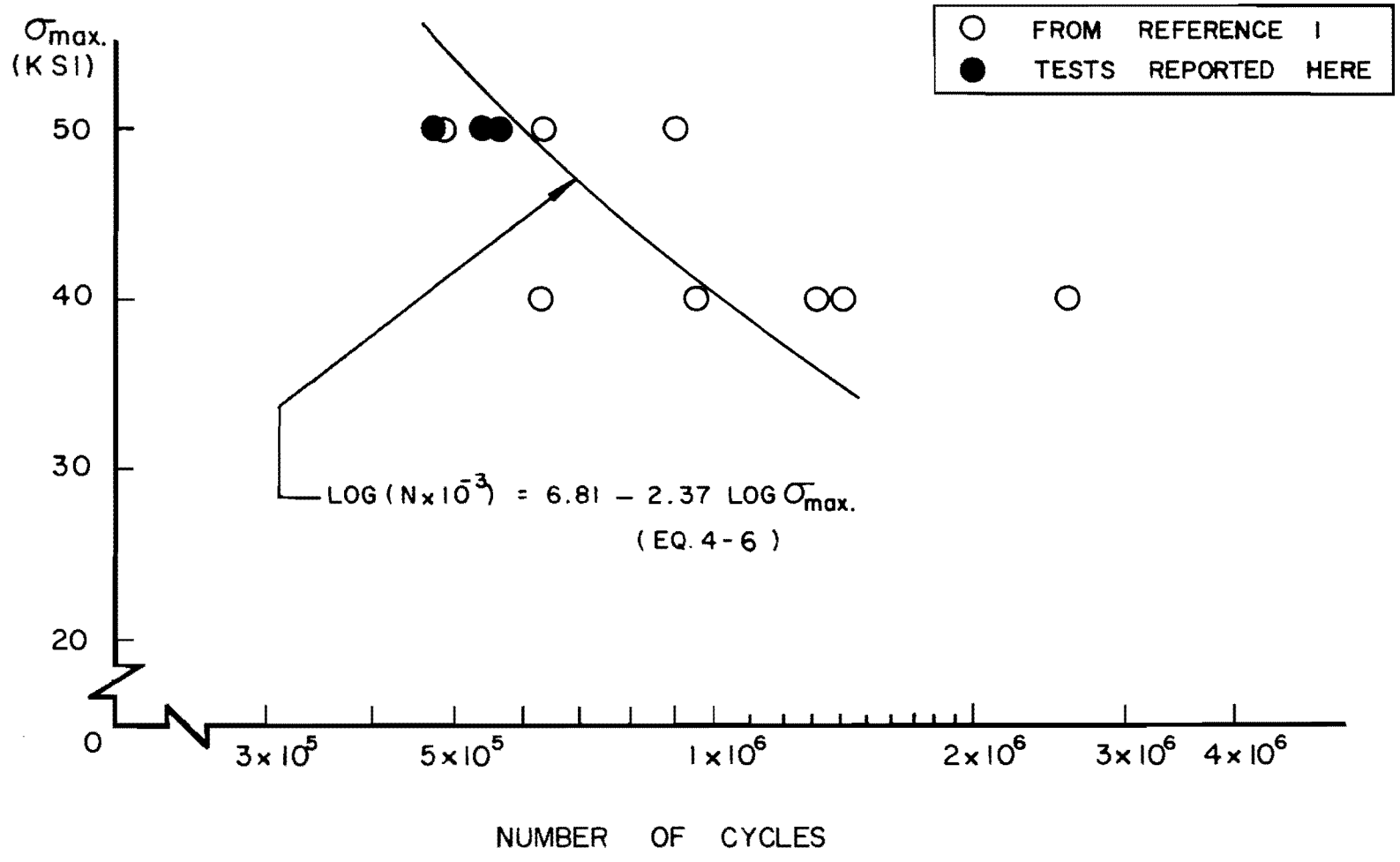

FIG. 29 RESULTS OF TYPE 3 CRACK